# Identification of three potential SPARC isoforms expressed by the larval fat body and wing imaginal discs and the requirement for the collagen-binding epitopes and the disulfide-bridged EF-hand2 for stereotypic BM assembly in *Drosophila melanogaster.*

by

Sebastian Duncan

A thesis submitted in conformity with the requirements
for the degree of Masters of Science

Cells and Systems Biology
University of Toronto

# Identification of three potential isoforms SPARC expressed by the larval fat body and wing imaginal discs and a requirement for the collagen-binding epitopes and the disulfide-bridged EF-hand2 for stereotypic BM assembly in *Drosophila melanogaster.*

Sebastian Duncan

Masters of Science

Cells and Systems Biology
University of Toronto

2019

## Abstract

The assembly of basement membranes (BMs) into thin sheet-like extracellular matrix networks with tissue-specific thicknesses is poorly understood. Loss of dSPARC results in 2nd instar larval lethality characterized by a fibrotic-like accumulation of Collagen IV surrounding the fat body adipocytes and retention in large vesicle-like structures during 2nd instar. Fat body-derived dSPARC and Collagen IV are co-secreted and localized on the surface of distal tissues. Stereotypic BM assembly is dependent on the conservation of the Collagen-binding epitopes and the disulfide bridge EF-hand2 of fat body-derived dSPARC. Imaginal wing disc-derived dSPARC fails to localize with Collagen IV-rich matrices, indicating that distinct isoforms of dSPARC are expressed by different tissues. Intracellular dSPARC and human SPARC yielded a novel 67 kDa isoform. The data provides the first *in vivo* evidence of three different isoforms of dSPARC, with potentially distinct functions in BM assembly and larval survival in *Drosophila.*

# Contents

# List of Figures

# 1 Introduction

Basement membranes (BMs) are specialized sheet-like extracellular matrices (ECMs) that underlie the basal side of epithelial sheets, surround adipocytes, muscle fibers, neurons and the lens capsules. Their diverse functions include epithelial morphogenesis, tissue barriers, adhesive surfaces for cell migration, and growth factor sequestration - reflective of their diverse tissue-specific functions throughout the development of complex animal forms (Jayadev & Sherwood, 2017; Kalluri, 2003). Consequently, mutations, ectopic overexpression, aberrant post-translational modifications, and autoimmune responses that affect the structural integrity of BMs are the underlying cause of lethal pathologies, such as Alport Syndrome, Thin-Basement Membrane Disease (TBMD), Epidermolysis Bullosa, Diabetes, and vascular defects (Jayadev & Sherwood, 2017).

BMs are composed of four core components: Laminin, Collagen IV, Perlecan and Nidogen. Significant progress has been made in our understanding of their synthesis, secretion and complex assembly and functions in BMs. However, proteomic studies indicate that the BM-tool kit is very complex, with approximately 100 non-core components identified in mammals with overlapping and distinct tissue-specific distributions (Jayadev & Sherwood, 2017). One non-core component is SPARC, a small calcium- and Collagen IV-binding glycoprotein. SPARC first appeared in Cnidaria, the first animal to form proper tissues with their ectoderm and endoderm associated with stereotypic BMs. Insight into the potential functions of SPARC in BM have been mainly derived from *in vivo* studies in *Caenorhabditis elegans* and *Drosophila melanogaster*. In addition to their genetic malleability, their BMs share many structural and functional similarities with vertebrate BMs. Moreover, their BMs represent the majority of their ECMs, facilitating analyses of data in a context not influenced by interactions and cross-communication with complex interstitial matrices.

The introduction first focuses on the structure of Laminin and Collagen IV and how their ability to self-assemble contributes to the formation of the polymeric networks of BMs. Secondly, the contribution of Perlecan and Nidogen to BM polymerization and homeostasis. Thirdly, how studies with invertebrate organisms have given novel insights into the functional relationship

between SPARC and Collagen IV. Finally, an overview of key aspects of fat body and wing imaginal disc development and BM dynamics, the experimental models used in my study.

## 1.1 Laminin structure, polymerization and functions.

Laminins are cross-shaped heterotrimers composed of α, β, and γ subunits. The genomes of *C. elegans* and *D. melanogaster*, code for two α subunits and one β and one γ subunit that combine to form two distinct heterotrimers (Domogatskaya et al., 2012). In mammals, five α, four β, and three γ chains have been identified, assembling into 16 heterotrimeric complexes that are often expressed and assemble into tissue-specific combinations (Domogatskaya et al., 2012). Laminin initiates the formation of the BM through its assembly into a polymeric network. *In vitro* studies have shown that Laminins can self-assemble into $Ca^{2+}$-dependent oligomeric complexes via the $NH_2$-terminal globular domains of their short arms (Domogatskaya et al., 2012). However, *in vivo,* the assembly is dependent and orchestrated by binding to integrin and dystroglycan transmembrane receptors (Li et al., 2017). Diverse functions of Laminin networks include cell polarity, tissue formation and adhesion, cell fate specification, and cell migration (Urbano et al., 2011).

In mammals, Laminin polymerization is largely initiated on cell surfaces immediately upon secretion. However, in some cases, a subset of Laminins diffuse to and are incorporated into BMs at distal sites. An example of this is observed in *Mus musculus*, where a Laminin containing an $\alpha_5$ subunit found in the neural tube is not expressed by neural tube cells (Jayadev & Sherwood, 2017). In *Drosophila,* a subset of Laminin derived from the fat body diffuses to and is incorporated in the BM of wing imaginal discs (Inoue and Hayashi, 2007). Similarly, *C. elegans* Laminin sub-lateral nerves contain a Laminin-$\alpha_2$ despite not expressing this α-chain (Jayadev & Sherwood, 2017). The extracellular deposition of Laminins is observed very early in development. Due to its indispensable role in BM assembly and function, mutations in Laminin-111 results in early embryonic lethality in vertebrate and invertebrate organisms, largely resulting from compromised epithelial morphogenesis (Jayadev & Sherwood, 2017).

## 1.2 Collagen IV structure, self-polymerization and integration into Laminin polymeric networks.

Collagen IV represents approximately 50% of the proteinaceous content of BMs (Kalluri, 2003), forming a polygonal network that functions to endow BMs with a tensile strength sufficient to protect tissues from biomechanical stress and serve as important regulators of cell-adhesion, signaling, and survival. Organisms expressing mutant forms of Collagen IV exhibit morphological deformities that often result in their developmental arrest during embryogenesis (Borchiellini et al., 1996; X. Guo et al., 1991; Gupta et al., 1997; Kelemen-Valkony et al., 2012; Kiss et al., 2016; Kuo et al., 2012; Maurer et al., 1995; Poschl, 2004; Sibley et al., 1994).

Collagen IV protomers are trimers composed of three α chains, tightly coiled into right-handed helices. The collagenous domains are composed of Gly-X-Y repeats where X and Y can be any amino acid, with proline and hydroxyproline are being frequently found at the Y position. The *Drosophila and C. elegans* genomes code for a Collagen IV α1 and α2 chain that give rise to a single heterotrimer composed of two α1 chains and one α2 chain. Collagen IV protomers are 400 nm-long trimeric helical proteins composed of an N-terminal domain (7S), an intermediate series of Gly-X-Y repeats interspersed with non-helical regions, and a large globular C-terminal domain (NC1) (Chioran et al., 2017).

The synthesis and proper folding of Collagen IV protomers is dependent on multiple complex processes within the ER. An N-terminal signal peptide ensures the co-translational insertion of Collagen IV α-chains into the ER lumen. In vertebrates, a Collagen-specific ER molecular chaperone, Hsp47, preferentially binds to properly folded triple helices of Collagen IV. Studies indicate that Hsp47 is not required for trimerization of Collagen α-chains but rather stabilizes protomers while in the ER and during their transit to the cis-Golgi (Koide et al., 2002; Ono et al., 2012; Tasab et al., 2000). *Hsp47*-null mice exhibit Collagen IV retention in dilated ER compartments as well as reduced Collagen IV incorporation in BM. The resultant Collagen IV network is also compromised as evidenced by an increased susceptibility to protease digestion. The absence of Hsp47 has no impact on the deposition of Laminin and nidogen during early stages of BM formation, consistent with its role as a Collagen-specific chaperone (Yasuhiro Matsuoka et al., 2004). However, as development progresses, the integrity of Laminin and fibronectin networks are compromised, underscoring a critical need for proper Collagen IV network

formation in BMs when embryos are undergoing muscular movements. The genomes of *C. elegans* and *Drosophila* do not code for Hsp47 (Chioran et al., 2017). It therefore remains to be established if a protein with chaperone-like properties exists that can substitute for Hsp47 in invertebrates.

Upon secretion, Collagen IV protomers polymerize into a mesh-like network. The globular noncollagenous C-terminal domain (NC-1) dimerizes, while N-terminal domains (7S domain) form antiparallel, laterally associated tetramers. Studies indicate that the first phase of polymerization involves the formation of non-covalently linked C-terminal dimers that are subsequently stabilized by lysyl oxidase-iron dependent catalyzed sulfilmine bonds (H. F. Guo et al., 2018). The 7S tetramer is mainly stabilized by disulfide bonds and lysyl oxidase cross-linking. The combination of N- and C-terminal cross-linking imparts tensile strength to the Collagen polymers. Lateral associations are also formed between the flexible intermediate collagenous domains; however, their precise contribution to Collagen IV extracellular assembly and mechanical stability is poorly understood.

As with Laminins, the location of Collagen IV synthesis is in some organisms distant from the site of its incorporation into BM; known examples include *Drosophila* and *C. elegans*. Thus, mechanisms must exist that delay immediate polymerization upon secretion *in vivo*, allowing for their diffusion or transport to distal sites. Data from our laboratory and others present the novel concept that the matricellular glycoprotein SPARC functions as an extracellular chaperone-like protein to ensure proper spatial assembly of Collagen IV in BM at proximal and distal sites (Isabella & HorneBadovinac, 2015; N. Martinek et al., 2016; Pastor-Pareja & Xu, 2011; Shahab et al., 2015).

## 1.3 Structure and function of Perlecan and Nidogen in BM.

Perlecan is a large heparan sulfate proteoglycan composed of a 500 kDa core protein and three 65 kDa N-terminal heparan sulfate glycosaminoglycan chains (Gubbiotti et al.,2017). Multiple functions have been ascribed to Perlecan, including vascular homeostasis, neurogenesis, growth factor sequestration and signaling. In *Drosophila*, Collagen IV recruits Perlecan (Trol) to BMs and postulated to counter the constrictive force provided by Collagen IV, thereby affecting tissue and cell shape. Lindner *et al.* demonstrated that Perlecan acts to sequester and activate

Decapentaplegic (a Transforming Growth Factor family member), Wingless (a Wnt growth factor) and Hedgehog, essential for second instar brain development. The authors also hypothesized that Perlecan interaction with PVF (PDGF and VEGF-like factor) promotes plasmatocyte proliferation (Lindner et al., 2007).

Nidogen is a 150 kDa glycoprotein composed of three globular domains, thought to link and stabilize the interactions between Laminin, Collagen IV and Perlecan. In mice, loss of nidogen leads to perinatal lethality due to multiorgan failure. In *Drosophila*, mutations in Nidogen do not impact organogenesis or BM formation but rather augment loss of Laminin and Perlecan phenotypes. Thus, the precise role of nidogen in BMs remains poorly understood (Dai et al., 2018).

## 1.4 Structure and function of SPARC in Collagen IV homeostasis in BM.

SPARC (Secreted Protein, Acidic, Rich in Cysteine)/osteonectin/BM40, a 32 kDa multifunctional $Ca^{2+}$ and Collagen-binding matricellular glycoprotein, is the founding member of the SPARC family. As with other members of the matricellular superfamily, SPARC is a transient component of interstitial ECMs and BMs. In vertebrates, SPARC levels become highest during tissue histogenesis, decreasing to basal levels once tissues have formed and reactivated in tissues undergoing remodeling or repair (Brekken & Sage, 2000; Lane & Sage, 1994; Nathalie Martinek et al., 2002; Ringuette et al., 1992; Schwarzbauer & Spencer, 1993). In triploblastic organisms, SPARC consists of three structural domains: an N-terminal high capacity, low-affinity $Ca^{2+}$-binding acidic domain (Domain I), a follistatin-like domain (Domain II) and an extracellular domain (EC-Domain III) (Koehler et al., 2009). Domain I is absent in diploblastic organisms.

The glutamic acid-rich Domain I can bind up to 8 $Ca^{2+}$ ions with low affinity (KD $Ca^{2+}$ = $10^{-3}$ to $10^{-5}$ M for vertebrate SPARC). Since it was first extracted from mineralized tissues, SPARC was termed osteonectin. However, it rapidly became clear that SPARC is highly expressed in non-mineralized tissues and is present in bone prior to the onset of mineralization. Despite its affinity for $Ca^{2+}$ ions, its function in bone remains elusive as SPARC-null mice mineralize properly. Hence the precise *in vivo* function of Domain I in triploblastic organisms remains unresolved. Domain I is absent from diploblastic organisms (Koehler et al., 2009).

The follistatin-like Domain (II) is comprised of 11 conserved cysteine residues, with one glycosylation site conserved among all trophoblast organisms, and is responsible for stabilizing the EF-hand1 found in the N-terminal region of Domain III (Koehler et al., 2009).

Domain III is the most evolutionary conserved domain for SPARC. It contains two low-capacity, high-affinity $Ca^{2+}$ binding EF-hands (*Drosophila* SPARC EF-hand1 at positions 233-262 and EF-hand2 at positions 266-295). It also contains two Collagen-binding epitopes (*Drosophila* SPARC, positions 182-189 and 260-264). $Ca^{2+}$ binding to the EF-hands is thought to induce a conformational change that augments $Ca^{2+}$-dependent Collagen-binding to SPARC. Domain III also binds to and inhibits PDGF and VEGF signaling (Cydzik et al., 2015). EF-hand1 is stabilized by an interaction with the follistatin-like Domain II, whereas the C-terminal EF-hand2 is stabilized by a disulfide bridge, the latter is a unique feature to the SPARC family and a small subset of other proteins (Nathalie Martinek et al., 2002). Biochemical studies demonstrate that a mutation in the disulfide bridge of EF-hand2 decreases $Ca^{2+}$ affinity and SPARC secretion (Pottgiesser et al., 1994).

Four potential SPARC binding sites have been identified on human Collagen IV (Hohenester, Sasaki, Giudici, Farndale, & Bächinger, 2008; Mayer, Aumailley, Mann, Timpl, & Eengel, 1991) Insight into a chaperone-like role for SPARC with respect to the assembly and maturation of Collagen IV in BMs has been primarily derived from invertebrate genetic model organisms. During *Drosophila* embryonic and larval development, dSPARC (*Drosophila* SPARC) is secreted principally by circulating hemocytes and the fat body (Nathalie Martinek et al., 2002), whereas in *C. elegans*, cSPARC (*C. elegans* SPARC) is secreted exclusively by body wall muscle cells, sex muscle cells, and the gonads (Fitzgerald & Schwarzbauer, 1998; Schwarzbauer & Spencer, 1993). In both organisms, SPARC appears to concentrate in BMs throughout the organism. Even though dSPARC and Collagen IV are colocalized within intracellular vesicles of *Drosophila* circulating hemocytes and fat body adipocytes, Collagen IV synthesis and secretion from cells are not affected by an absence of SPARC (Isabella & Horne-Badovinac, 2015; Pastor-Pareja & Xu, 2011; Shahab et al., 2015). Knockdown of dSPARC in the *Drosophila* fat body leads to the rounding of polygonal adipocytes and their encapsulation by a thick fibrotic-like accumulation of Collagen IV and the other core BM components (Shahab et al., 2015). A similar phenotype was reported by Pastor-Pareja and Xu (Pastor-Pareja & Xu, 2011) with the additional observation that the loss of fat body-derived SPARC led to an absence of Collagen IV, but not Laminin, in the BM of wing

imaginal discs, which do not synthesize Collagen IV (Pastor-Pareja & Xu, 2011). Perlecan deposition at the distal tissues was also reduced as a result of decreased Collagen IV assembly (Pastor-Pareja & Xu, 2011). This striking phenotype indicates that SPARC is essential for permitting Collagen IV to diffuse from sites of production and assemble on the surfaces of distal tissues. Supporting evidence for this also exists in *C. elegans*, where cSPARC is required to ensure that Collagen IV derived from the body wall muscle cells diffuses to, and is incorporated into, the BM of distal pharyngeal tissue (Morrissey et al., 2016). In the absence of SPARC, Collagen IV assembles and accumulates on the surface of the cells that synthesize it rather than diffusing to distal sites (Pastor-Pareja and Xu, 2011). It is likely that an optimal amount of SPARC is produced to regulate Collagen IV solubility, thereby ensuring that an appropriate amount of Collagen IV is permitted to diffuse to secondary sites, while allowing polymerization of a subset of Collagen IV at the site of secretion.

The deposition of Collagen IV by the *Drosophila* egg follicle enables the morphological development of the oocyte within the egg chamber. The increased tensile strength associated with Collagen IV deposition begins to constrict stage 6 egg chambers to promote their transformation from a spherical to an ellipsoidal morphology by stage 10 (Isabella & Horne-Badovinac, 2015). A dramatic decrease in dSPARC mRNA levels occurs at stage 5 of normal egg chamber development which is coincident with an increase in Collagen IV deposition into the follicular BM surrounding the egg chamber (Isabella & Horne-Badovinac, 2015; Nathalie Martinek et al., 2002). Consistent with the theory that Collagen IV solubility is enhanced by SPARC, overexpression of dSPARC led to a decreased amount of Collagen IV present in the follicular BM and retention of a spherical morphology (Isabella & Horne-Badovinac, 2015). The authors postulated that dSPARC functions as a chaperone-like molecule to regulate the solubility and nucleation of Collagen IV, which ensures appropriate tensile strength of the follicular BM to allow proper egg development.

Increased SPARC levels have been positively correlated with invasive behavior of a subset of solid tumors (Brown et al., 1999; Chen et al., 2012; Ledda et al., 1997; Rempel et al., 1999). Epithelial carcinomas must breach a surrounding BM for the invasive process to occur. Both metalloprotease-dependent and -independent processes have been implicated in facilitating transmigration of invasive cancer cells across the BM barrier into the surrounding stroma (Rowe

& Weiss, 2008). As with interstitial ECMs, BMs undergo continuous remodeling throughout normal and pathological development (Egeblad & Werb, 2002; Kelley et al., 2014; Medioni, 2005; Srivastava et al., 2007; Werb & Chin, 1998). It is possible that an elevated expression of SPARC by a carcinoma, over time, weakens the tensile strength of the BM during remodeling in a metalloproteinase-independent manner by affecting the deposition and assembly of newly-synthesized Collagen IV. Consistent with this possibility, during the development of the *C. elegans* reproductive system, anchor cells migrate through a BM to reach the underlying vulva cells, an event used as a model to study properties of invasive cells (Hagedorn & Sherwood, 2011). Morrissey et al. demonstrated that overexpression of cSPARC increases the invasive behavior of these anchor cells, an event coincident with the reduced rate of newly-synthesized Collagen IV incorporation into the juxtaposed BM (Morrissey et al., 2016). Thus, data derived from invertebrate organisms are consistent with the hypothesis that SPARC serves as an extracellular chaperone during the nucleation phase of Collagen IV assembly in BMs and has important implications for vertebrate physiology and pathology.

Current evidence strongly supports the notion that binding of SPARC to collagen IV is likely required to regulate the timely nucleation of Collagen IV, preventing the aggregation of prematurely formed Collagen IV networks that can entrap other BM components at the site of secretion. If SPARC is necessary to maintain Collagen IV solubility in the extracellular space, it would be advantageous for SPARC and Collagen IV to associate just prior to their exit from the cell to ensure their co-secretion. Unpublished data from our laboratory suggest that dSPARC colocalizes with Collagen IV within the trans-Golgi network. One can envision that two distinct subsets of Collagen IV protomers exit the cell: a subset of Collagen IV secreted bound to dSPARC and a second subset secreted without dSPARC. The subset bound to dSPARC is expected to be more soluble than unbound Collagen IV and its polymerization would be sufficiently delayed, permitting its diffusion to distal tissues. The Collagen IV protomers secreted without dSPARC would be polymerized into a BM at the site of secretion. While dSPARC and Collagen IV were co-localized in most large secretory vesicles of *Drosophila* embryonic hemocyte-derived cells *in vitro*, a subset had no visible co-localization (unpublished data). The nucleation phase of this population of Collagen IV is expected to be more rapid and would polymerize into BMs at the site of secretion. *In vitro* kinetic studies with purified Collagen IV protomers in the absence and presence of SPARC are required to validate this hypothesis.

## 1.5 SPARC may also function as a Collagen IV extracellular chaperone-like protein in vertebrates.

Evidence for the impact of SPARC on Collagen IV assembly and maturation in vertebrates is more limited compared to that for fibril-forming Collagen I (Bradshaw, 2009). In vertebrates expressing other members of the SPARC family, loss of SPARC is not embryonically lethal (Gilmour et al., 1998). However, in mice, knockout of SPARC results in postnatal age-onset of cataract formation in the lens capsule (Norose et al., 1998) and loss of Collagen-fibril tensile strength in the dermis (Rentz et al., 2007). The lens capsule is a specialized BM composed of a complex mixture of macromolecules, including Laminin, Collagen XVIII, Perlecan, Nidogen, Fibronectin, and Collagen IV (Danysh & Duncan, 2009; Kelley et al., 2014). Six Collagen IV α-chains (α1-α6) are expressed by lens capsule cells that give rise to three protomer isoforms (α1α1α2, α1α2α5α6, and α3α4α5) which assemble into three stage-specific Collagen IV networks with distinct biomechanical properties (Danysh & Duncan, 2009). Lens capsule BM components are secreted by the anterior lens epithelial cells and the lens fiber cells, whose nuclei reside in the equatorial region of the lens with cytoplasmic extensions towards the posterior end of the lens capsule. While SPARC is expressed by both the epithelial cells and fiber cells, it is not detected within the lens capsule BM (Yan et al., 2002). Nonetheless, in the absence of SPARC, the integrity of the lens BM is compromised, and long cellular protrusions of the underlying epithelia are visible in the BM (Norose et al., 1998; Yan et al., 2002). The severity of BM disorganization is not circumferentially uniform but is more prominent in the posterior end (Yan et al., 2002). Unlike the anterior and equatorial regions of the capsule, which are in direct contact with the lens epithelial cells or differentiated fiber cells, the posterior end is only partially contacted by the cytoplasmic extensions of fiber cells. Thus, the formation of the posterior lens BM may be dependent on the diffusion of BM components from the anterior and lateral sites of production. We propose that, in the absence of SPARC, the solubility of Collagen IV produced by the anterior and lateral cells is likely impeded, reducing the ability of Collagen IV to diffuse and polymerize on the posterior end of the lens capsule. Laminin also accumulates in the lens BM of SPARC-null mice (Yan et al., 2005). The accumulation of BM components and compromised biomechanical integrity in *SPARC*-null mice lens capsules is consistent with a role for SPARC in Collagen IV nucleation and BM homeostasis, as indicated with invertebrate studies. In the African clawed frog, *Xenopus laevis*, the knockdown of SPARC with high levels of anti-sense morpholino leads to

developmental arrest at the end of gastrulation, well before the onset of organogenesis when BMs are assembled (Huynh et al., 2011). However, injection of low levels of SPARC anti-sense morpholino, which do not inhibit organogenesis, phenocopies the formation of lens cataracts like those observed in SPARC-null mice (Huynh et al., 2011).

## 1.6 Drosophila fat body development and BM.

The *Drosophila* fat body is a mesoderm-derived organ that is often referred to as the equivalent of the mammalian liver. However, the fat body is an endocrine organ responsible for the majority of hemolymph proteins and organic compounds whose functions include hormone signaling, growth regulation, nutrient sensing, energy metabolism and innate immune response (Palli and Locke, 1988). Development of the *Drosophila* fat body begins at embryonic stage 11/12 from 9-bilateral columns of progenitor cells derived from the inner layer of the mesoderm. The progenitors are present within the inner layer of the mesoderm, spanning parasegments 4 through 12. During stage 13, the bilateral clusters of fat body columnar precursors are transformed into elongated sheets of cells located between the developing visceral musculature and the body wall (Hoshizaki *et al.*, 1994, 1995; Riechmann *et al.*, 1998). By late stage 15/16, a single-cell thick fat body has been transformed within the abdomen into three morphological domains: the lateral fat body, the dorsal fat-cell projections and ventral commissure. By the end of embryogenesis (stage 17), the fat body is completely developed and comprises of approximately 2200 adipocytes that remain constant in number and begin to undergo endoreplication and increase in volume during larval development (Butterworth et al., 1988; Britton and Edgar, 1998; Hackl *et al.*, 2005). Between 1$^{st}$ instar and the end of the 3$^{nd}$ instar, the polygonal adipocytes undergo a 200-fold increase in volume from the beginning the 1$^{st}$ instar. The volume increase is in part due to the synthesis and storage of glycogen and triglyceride-rich vesicles, which serve as an energy source during the wandering stage and pupariation (Aguila *et al.*, 2007; Sam, Leise and Hoshizaki, 1996). During pupal development, the fat body undergoes a dramatic remodeling. Approximately 6 hours after pupariation, the adipocytes lose their polygonal shape as they begin MMP-dependent dissociation.

While contributing to some of the production of BM components during later stages of embryonic development, the fat body is the principal source of BM components during larval development (Shahab *et al.*, 2015). While bathed in hemolymph, the fat body is shielded from direct contact

with the hemolymph by an enveloping BM. The negatively charged BM serves as a filter to prevent the diffusion of positively charged macromolecules that are larger than 15 nm from the hemolymph. Adipocytes juxtaposed to the BM maintain a space between each other by the presence of an intercellular ECM rich-lymph and plasma membrane reticular network. Surface plasma membrane extensions by the adipocytes also further increase the surface area of the intercellular space. The intercellular space contains filtered lymph, thereby rendering it osmotically distinct from the hemolymph. Depending on the location of the adipocytes in the fat body, they will have different degrees of contact with the BMs. Irrespective of their location, adipocyte cell-cell adhesion is promoted in 3$^{rd}$ instar larvae by the presence of Collagen IV-Intercellular Concentrates (CIVICs) that are enriched in all universal BM components and dSPARC. Thus, the *Drosophila* fat body is an excellent model to study the functional relationship between dSPARC and Collagen IV synthesis and assembly in BMs.

## 1.7 Wing Imaginal Disc development and BM assembly

*Drosophila* adult wings develop from a bilateral pair of larval wing imaginal discs that originate during embryogenesis from a cluster of a few ectodermal cells. The embryonic cell clusters invaginate, with the apical domains of the disc cells facing the lumen. During larval development, the discs transform into flattened sacs composed of two separate cell layers, a columnar epithelium capped by a peripodial membrane composed of squamous cells. During early 1$^{st}$ instar development, wing discs are composed of a few dozen epithelial cells that continue to proliferate exponentially throughout larval development, such that by late 3$^{rd}$ instar, the wing discs are composed of approximately 50,000 cells (Beira and Paro, 2016). A BM derived from fat body adipocytes and wing disc columnar epithelial cells is bound to the basal surface of the columnar epithelium. Collagen IV and Perlecan are derived from the fat body adipocytes, whereas Laminin is synthesized by the fat body and wing imaginal discs (Inoue and Hayashi, 2007; Pastor-Pareja and Xu, 2011). Constriction by the BM is modulated by various proteins including integrins, MMPs, and dSPARC that collectively shape the *Drosophila* wing discs (Pastor-Pareja and Xu, 2011; Ma *et al.*, 2017). Bone morphogenetic protein/transforming growth factor β ligand is released into the hemolymph in the absence of the BM, resulting in smaller wings. However, loss of the BM has no effect on Hippo signaling, a pathway responsible for mechanosensing and tissue growth (Ma *et al.*, 2017). Thus, the wing imaginal disc serves as a excellent, accessible model to

gain a better understanding of the role of dSPARC in regulating BM assembly and dynamics during larval development in epithelial tissues.

# 2 Objectives

Five major objectives were undertaken to gain a better mechanistic understanding of the function(s) of dSPARC in *Drosophila* BM assembly and stability.

1. Transgenic expression of C-terminal tagged dSPARC with mCherry produces a non-functional fusion protein that is degraded. The objective was to determine if either GFP or HA C-terminal tagging could be used to produce a non-degraded functional fusion protein for a structure-function analysis.
2. Generate transgenic flies expressing dSPARC constructs with mutated Collagen-binding epitopes or disulfide bridge of EF-hand2 and assess their impact on BM assembly and stability.
3. In contrast to bone-derived human SPARC (hSPARC), platelet-derived hSPARC has no measurable affinity for Collagens. Therefore, the objective was to determine if dSPARC from different tissues co-localize with Collagen IV-rich ECMs.
4. Vertebrate studies have long raised the possibility of an intracellular form of SPARC (iSPARC). The fourth objective was to assess the impact of a dSPARC construct lacking the signal peptide (iSPARC) in a wild-type or *dSPARC*-protein null background on development.
5. In light of the striking evolutionary conservation of domain II-III from cnidarians to mammals, my final objective was to determine if hSPARC could rescue larval lethality associated with the absence of dSPARC.

# 3 Materials and methods

## 3.1 Mutant generation through gateway cloning

### SPARC Constructs

cDNA for SPARC constructs were synthesized using GeneArt Strings™ technology by ThermoFisher Scientific. PCR amplification of cDNAs encoding for *dSPARC*, *hSPARC* (human SPARC), $dSPARC^{mCBD}$ (dSPARC with a mutated Collagen-Binding Domain), $dSPARC^{mDB}$ (dSPARC with a missing Disulfide bridge EF-hand2), and $dSPARC^{\Delta SP}$ (dSPARC with a deleted Signal Peptide), generated amplicons of the appropriate molecular weights. PCR amplification consisting of 45 cycles of denaturing (94$^{o}$C for 30 sec), annealing (60$^{o}$C for 1 min) and extending (70$^{o}$C for 1 min) was done adding *NotI* (5'-GCGGCCGC-3') and *SalI* (5'GTCGAC-3') digestion sites at the ends of the DNA constructs.

### Digestion of SPARC constructs and pENTR vector

The pENTR 2B Dual selection vector obtained from ThermoFisher Scientific and PCR-constructs were separately incubated with *NotI* and *SalI* Fast digestion enzymes for 2 hr at 37°C. The digested products were incubated separately at 65°C for 20 min to inactivate the fast digestion enzymes. A gel extraction kit was used to extract and purify the product, in preparation for ligation. *NotI* and *SalI* digestion of PCR products yielded single bands of similar molecular weight to the undigested PCR product, with no visible degradation the digested pENTR vector yielded a 2.3 kb band (Figure 1).

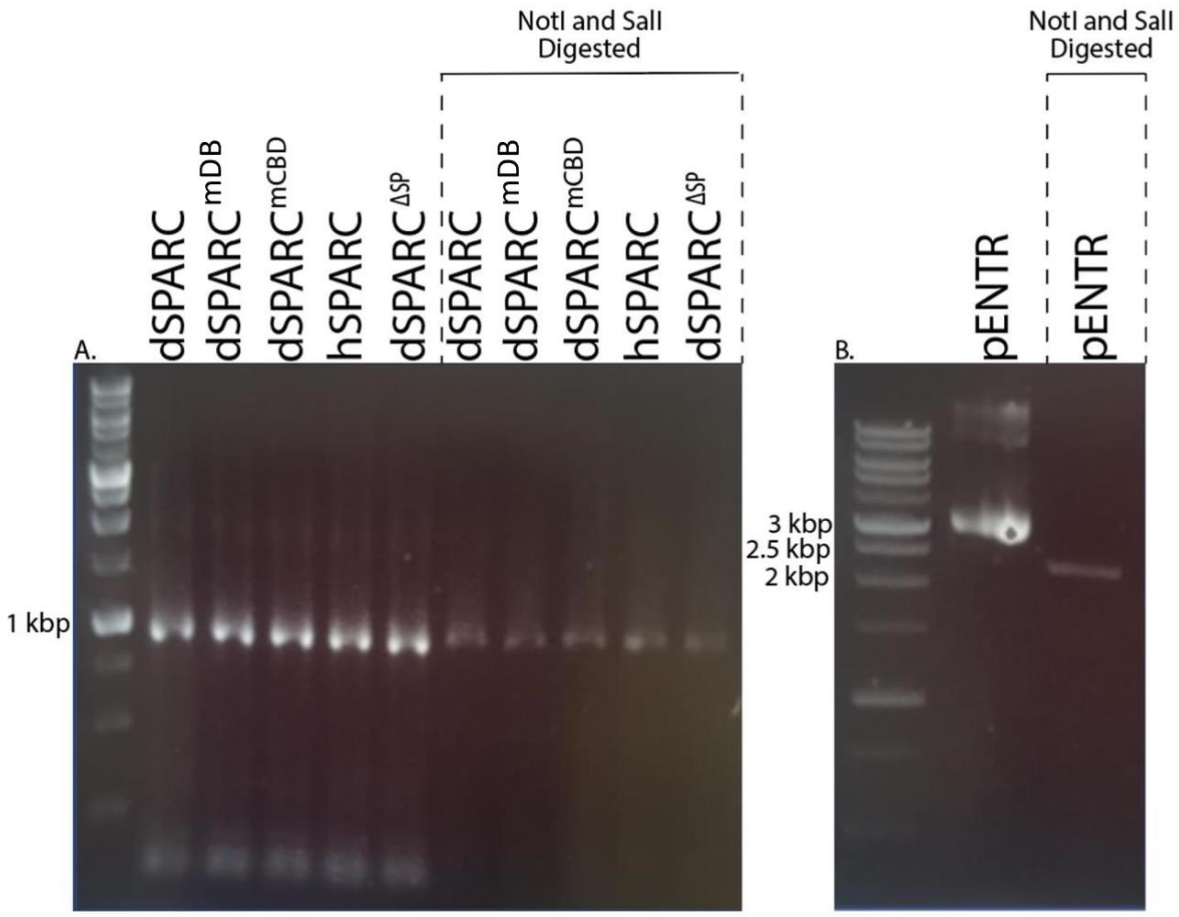


**Figure 1. Digestion of PCR fragments and pENTR vector with *NotI* and *SalI*.**

**A.** PCR amplified SPARC fragments before and after digestion with *NotI* and *SalI*. The size of the fragments corresponds to the expected molecular length expected from dSPARC cDNA. **B.** pENTR vector before and after *NotI* and *SalI* digestion. A single band of 2.3 kb is observed indicative of a complete digestion.

## *SPARC* cDNA ligation into pENTR

The extracted products were combined at a 3:1 insert to vector ratio at 4°C overnight with DNA ligase. The newly ligated vector, known as the entry clone, was then used to transform in DH5α E. coli cells, and grown in a kanamycin medium to select against non-ligated vectors.

## Recombination of entry and destination vector

The isolated entry vector, containing the desired SPARC construct, was recombined with a vector containing the UAS promoter and a C-terminus HA tag (pPWH vector). 100 ng of the entry vector, 150 ng of the pPWH vector and 2 µL of LR clonase II enzyme were incubated at 25°C overnight to achieve recombination. To terminate the reaction Proteinase K was added at 37°C for 10 min. The product was then transformed in TOP10 cells and grown in ampicillin plates, thereby selecting against non-recombined vectors that carry a CCdB lethal gene. The vector was then isolated and ran in an agarose gel (Figure 2).

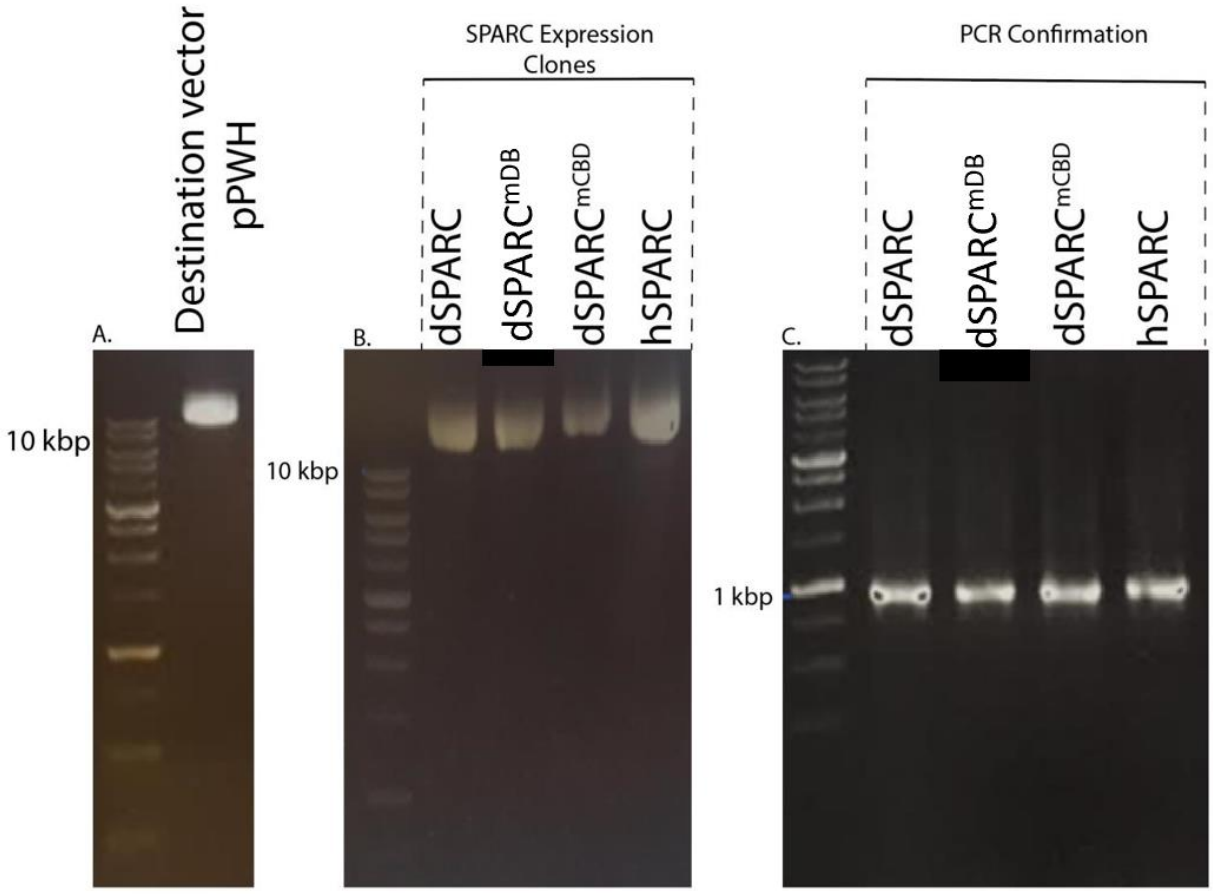


**Figure 2. Recombination of pENTR *SPARC* containing the *SPARC* cDNA into the gateway destination vector (pPWH).**

**A**. Gateway pPWH vector. **B.** Destination vector; *dSPARC*, *dSPARC* with mutated Collagen binding sites (*dSPARC*$^{mCDB}$) dSPARC without a disulfide bridge (*dSPARC*$^{mDB}$), and human SPARC (*hSPARC*). **C**. PCR confirmation that SPARC-pPWH expression clones, contain a 1 kb band corresponding to SPARC cDNA.

## Selection and balancing of transgenic lines

White-eye flies were injected with the expression clone. Selection for the mini-white marker (orange eye) was performed. Selected flies were crossed with a double-balanced line (Bl/CyO;TM2/TM6B) and made homozygous. Diagram 1 shows an overview of the genetic modifications in each line.

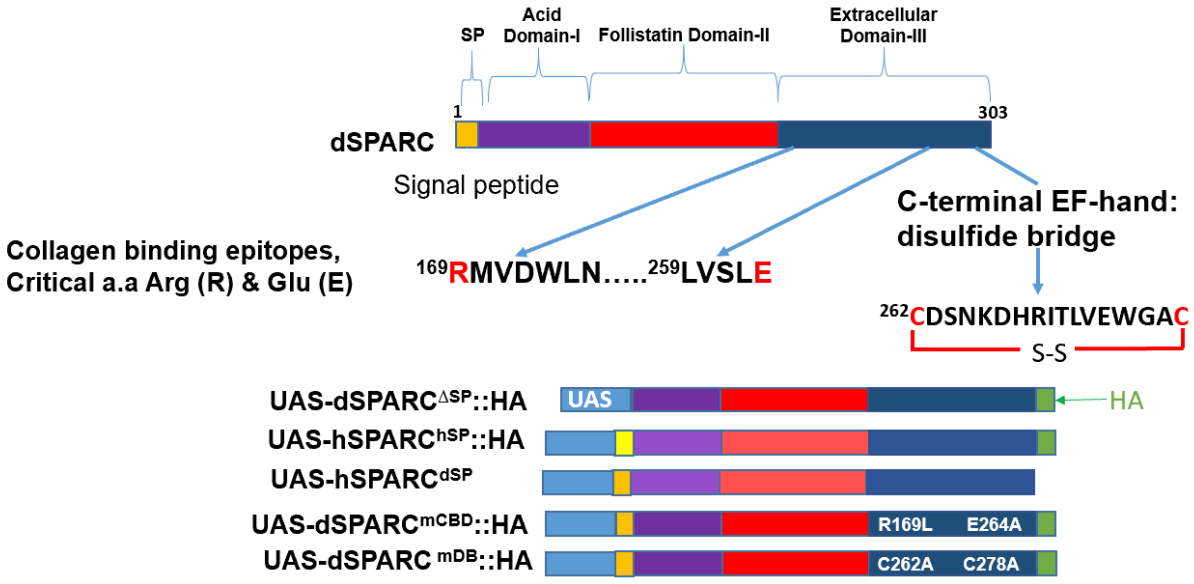


**Diagram 1.** Schematic representation of SPARC transgenic constructs generated via gateway cloning. The schematic indicates UAS (light blue), a signal peptide (yellow and orange), Domain I (purple), Domain II (red), and Domain III (dark blue). Mutated amino acids in Domain III are highlighted.

## 3.2 Fat body and wing imaginal disc analysis

### Fat body Isolation

3rd instar larval with the desired genotype were placed in a dissection well containing 1xPBS. The forceps are used to make an incision tearing the abdominal epidermis. The posterior end is the then held by one set of forceps and, using the other forceps, the cuticle is slid along. The same thing is done using in the anterior end, effectively removing the cuticle of the larval. The fat body is then separated from all other tissues and prepared for immunostaining or western blot (W.B) analysis.

### Western blot

The desired tissue was lysed in lysis solution (100 mM tris 4% SDS pH 6.8), and protein concentration was measured using the bicinchoninic acid assay (BCA assay). 5-20 µg of each sample was loaded into 4-20% SDS-page gel and ran for 1 hr at 100 mV. Proteins were transferred from the SDS-PAGE gels to PVDF membranes at either 20 mV/100 Amps over night or 100 mV/250 Amps for 1 hr. The membrane was blocked for 1-2 hrs with blocking solution (PBS containing 0.1% Tween 20 and 5% skim milk). The blot was then placed in fresh blocking solution with primary antibody overnight at 4°C. After washing the membrane was incubated 12 hrs with a peroxidase-conjugated secondary antibody. The washed membrane was exposed to chemiluminescent reagents (Santa Cruz Catalog # SC-2048). Membranes were visualized using BioRad Molecular Imager Gel Doc™ XR+ Imaging System.

### Confocal and spinning discs preparation and imaging

Tissue samples were fixed with 4% paraformaldehyde, blocked with 5% donkey serum for 30 mins, and then incubated with the primary antibody overnight at 4°C. The tissue was washed and blocked again for 1 hr. Alexa Fluor conjugated secondary antibodies were added to the solution and incubated for 2 hr. Tissue samples were placed on a slide and protected using Vector shield mounting medium. All preparations were then imaged using a confocal microscope or spinning disc. Image analysis was done using ImageJ (FIJI).

| **Antibody** | **Host** | **Dilution (used for W.B and confocal)** |
|---|---|---|
| Anti-dSPARC | Rabbit | 1:1000 |
| Anti-tubulin (E7) | Mouse | 1:500 |
| Anti-HA | Mouse | 1:1000 |
| Anti-rabbit HRP | Donkey | 1:2500 |
| Anti-dSPARC | Rabbit | 1:1000 |
| Anti-Laminin b1 | Rabbit | 1:500 |
| Anti-Cg25c | Guinea pig | 1:500 |
| Alexa 647 Anti-guinea pig | Donkey | 1:500 |
| Alexa 555 Anti-rabbit | Donkey | 1:500 |
| Alexa 488 Anti-mouse | Donkey | 1:500 |

## dSPARC lethality/rescue assay

UAS-*dSPARC*::HA generated mutants were screened and made homozygous through the mini-white eye marker. The mutants were then crossed to *dSPARC*-Gal4 and *dSPARC*$^{1510D}$, lines which do not express SPARC protein, to generate a *dSPARC*-protein null background set to be lethal in 2$^{rd}$ instar. The progeny was then assess, to examine if 2$^{nd}$ instar lethality could be rescue. Lethality/rescue was assessed by number and stage of larval death. The larvae was scored by the size of the mouth hooks and the shape of the spiracles.

## Adipocyte size growth of early 2$^{nd}$ instar to wondering 3$^{rd}$ instar

Adipocyte size was calculated by manually selecting the volume of adipocytes with the help of FIJI. Values for the size of early 2$^{nd}$ and wondering 3$^{rd}$ instar larvae were average and the 95% confident interval (95% CI) was calculated. 2$^{nd}$ and 3$^{rd}$ instar larval sizes were then compared for significance using the unpaired t-test (GraphPad Prism®).

### 3.1.1 Stocks

All stocks and genotypes can be found in the appendix 1A.

# 4 Results

The fat body is the major source of BM components during *Drosophila* larval development. Previous studies in the laboratory have demonstrated that dSPARC is a major component of larval fat body BM. Absence or KD of dSPARC is associated with 2$^{nd}$ instar lethality coupled with a fibrotic-like accumulation of Collagen IV in the BMs surrounding the fat body adipocytes. My main objective was to generate a series of transgenic fly lines expressing dSPARC mutations to identify which domains of dSPARC are critical for *Drosophila* BM homeostasis during larval development and determine if human SPARC can rescue an absence of dSPARC. Tagging of dSPARC with a fluorescent probe would offer several advantages, principal among an ability to image the spatiotemporal distribution of dSPARC in living cells in real time. Unfortunately, a previous study in the laboratory demonstrated that loss of dSPARC cannot be rescued by a transgenic *dSPARC::mCherry* fusion construct. Western blot analysis revealed that *dSPARC::mCherry* construct yields two protein bands, (1) at 27 kDa and (2) at 37 kDa, instead of a band at 64 kDa corresponding to the expected molecular weight of the fusion protein; indicating that the dSPARC::mCherry protein is cleaved intracellularly, producing a non-functional dSPARC protein (Scuric 2016). However, a study reported that C-terminal GFP-tagged SPARC is functional in *Caenorhabditis elegans* and localizes to BMs (Fitzgerald and Schwarzbauer, 1998). Moreover, studies by Sally Horneba-dovinac and Eduardo Moreno using a *UAS-dSPARC*::HA transgenic fly line indicate that C-terminal tagging of dSPARC with HA also generates a functional protein that impacts the levels and function Collagen IV in the BMs of several tissues. Hence, my first objectives were to determine if substituting the mCherry tag for GFP would yield a stable fusion product and confirming *dSPARC*::HA yields a fusion protein that localizes to larval fat body BM and can rescue *dSPARC*-deficient flies.

## 4.1 *dSPARC*::GFP is retained intracellularly in the fat body of 3rd instar larvae and fails to localize with adipocyte BM

A *dSPARC::GFP* line was obtained from VDRC, which codes transgenic *dSPARC*::GFP as well as the endogenous dSPARC copy on the 3rd chromosome. Western blot analysis revealed two bands; (1) a 65 kDa band corresponding to the expected molecular weight of dSPARC::GFP fusion protein, and (2) a 37 kDa band characteristic of endogenous dSPARC (Figure 3A). Thus, in contrast to dSPARC::mCherry, dSPARC::GFP is not degraded in *vivo*. As SPARC::GFP co-localizes with endogenous SPARC in BM of *C. elegans*, I therefore investigated if dSPARC::GFP co-localizes with endogenous dSPARC in fat body BMs. Unfortunately, dSPARC::GFP does not localize to the periphery of cells like WT in 3rd instar fat body, but is retained intracellularly in the fat body adipocytes (Figure 3B). Hence, the collective data indicate that a structural-functional analysis cannot be undertaken with a dSPARC::GFP fusion protein. I therefore shifted my attention to confirming that as reported, tagging dSPARC with HA generates a stable and functional fusion protein in *Drosophila.*

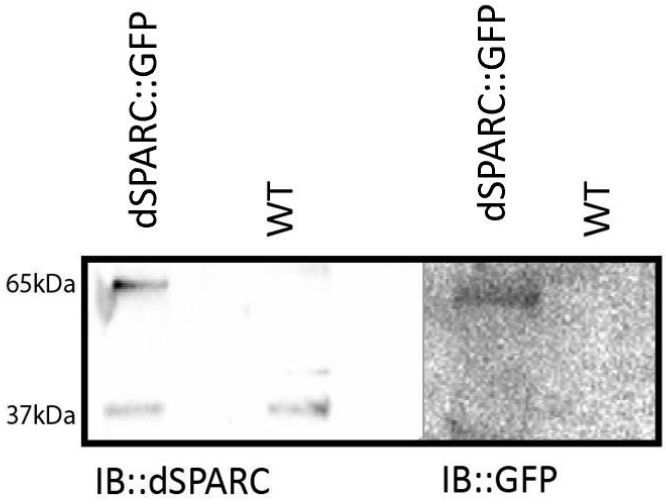
dSPARC::GFP
WT
dSPARC::GFP
WT
65kDa
37kDa
IB::dSPARC
IB::GFP

B. Fat body

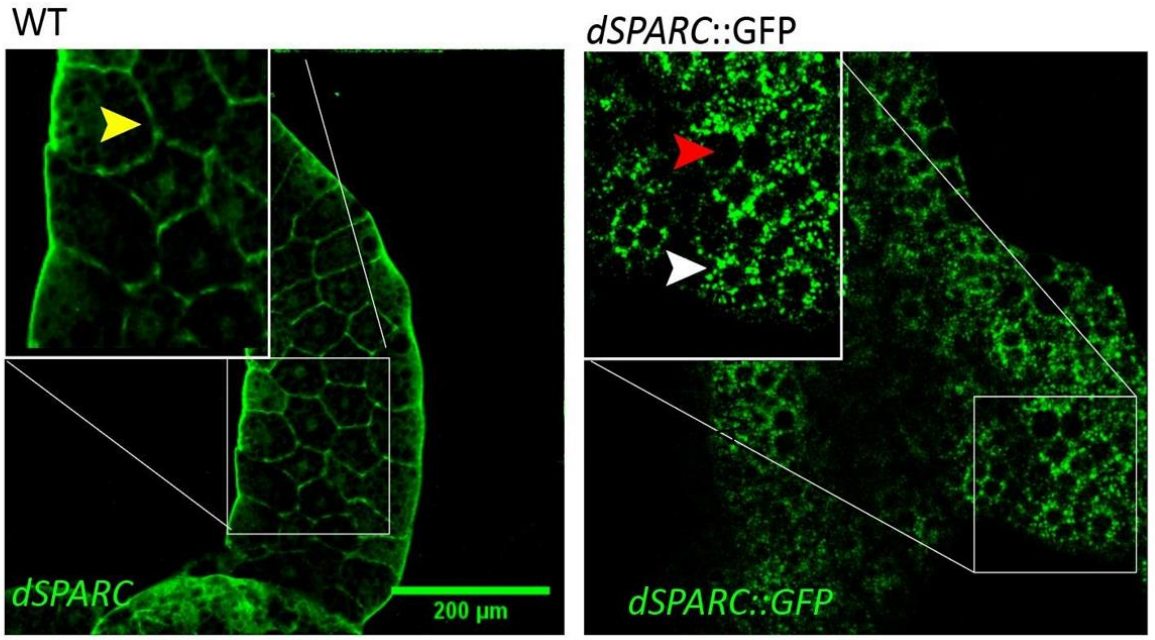
WT
dSPARC::GFP
dSPARC
200 µm
dSPARC::GFP

**Figure 3. Western blot and immunofluorescent analysis of dSPARC::GFP.**

**A.** Western blot analysis of dSPARC::GFP fly lysate isolated from adult *Drosophila* immunoblotted with either anti-GFP or anti-dSPARC antibodies. **Lane 1.** Immunoblotting with anti-GFP antibodies reveals a 65 kDa band corresponding to the expected molecular weight dSPARC::GFP. **Lane 2.** Immunoblotting for dSPARC reveals an additional 37 kDa band corresponding to the molecular weight of dSPARC. **B**. 3$^{rd}$ instar fat body immunostaining with anti-dSPARC antibody of wild-type reveals dSPARC border cell (yellow arrow) and nuclear-like staining. Immunofluorescent analysis of dSPARC::GFP shows punctate intracellular fluorescence (white arrow) surrounding lipid vesicles (red arrow), with no visible cell border.

## 4.2 *dSPARC*::HA is not degraded, localizes to larval fat body BM and rescues *dSPARC*-deficient flies to adulthood

A *UAS-dSPARC*::HA transgenic fly line was obtained from the lab of Eduardo Moreno (Portela, Marta, et al. 2010). Western blot analyses of the 3rd instar larval protein extracted from two fly lines [*Cg*-Gal4>UAS-*dSPARC*::HA (II) and *Cg*-Gal4>UAS-*dSPARC*::HA (III)], yielded a 37 kDa band, corresponding to the predicted molecular weight of the *dSPARC*::HA fusion construct (Figure 4A), with no visible lower molecular weight degradation products. Additionally, driving expression of UAS-dSPARC::HA with the *Cg*-Gal4 in a dSPARC WT background showed an increase in band intensity consistent with what would be expected with dSPARC overexpression (Figure 4A). Therefore, to test functionality and decrease the probability of potential overexpression phenotypes, I sought to drive expression of dSPARC::HA in a dSPARC deficient background. *dSPARC*-Gal4>UAS-UAS-*dSPARC*::HA (II) was able to rescue *dSPARC*-deficient animals (Df(3R)nm136) into adulthood. Moreover, a normal distribution of both *dSPARC*::HA and Collagen IV in 3rd instar larval fat body adipocytes was displayed by immunofluorescence microscopy (Figure 4b); in contrast to a *dSPARC* deficiency, which is associated with 2nd instar lethality and fibrotic accumulation of Collagen IV (Figure 3). Intriguingly, *dSPARC*-deficient and *dSPARC*-mutant flies rescued with the Cg-Gal4 driver failed on occasion to eclose from their puparium, whereas driving expression with *dSPARC*-Gal4 had no eclosion defects. Therefore, unless otherwise noted, all genetic crosses for the remainder of this thesis were carried out with the *dSPARC*-Gal4 line to drive transgenic expression of C-terminal HA-tagged *dSPARC::HA* constructs.

## 4.3 Adipocyte cell-cell adhesion is in part dependent on CIVICs in 3rd instar but not during early 2nd instar.

By the end of embryogenesis, the fat body is composed of approximately 2200 adipocytes that remain constant in number, but increase in volume, throughout larval development. It was therefore of interest to determine if changes in the distribution in the surrounding ECM (BM and CIVICs) are associated with a remarkable 200-fold increase in adipocyte volume from early 1st instar to wandering 3rd instar. The role of ECMs in 2nd instar fat body development is poorly understood largely due to technical challenge of extracting intact fat body from the small 2nd instar larvae, resulting in the vast majority of studies being carried out with much larger 3rd instar fat

body. To examine the spatiotemporal distribution of dSPARC and Collagen IV in 2nd instar fat body, no attempt was made to remove intact fat body from the larvae. Instead 2nd instar larvae were teared open to expose the fat body, which provided sufficient intact fat body tissue for immunofluorescent analysis.

A previous study identified a new structure called Collagen IV intracellular concentrations (CIVICs) critical for adipocyte cell-cell adhesion, with dSPARC overexpression leading to a partial adipocyte cell-cell detachment and a loss of Collagen IV in CIVICs. I now report that CIVICs are absent in early 2nd instar when adipocytes cells are approximately 1800 $\mu m^3$ (Figure 5A, B). However, CIVICs become visible by immunofluorescence microscopy in late 3nd instar fat body when adipocyte had undergone a 67-fold increase in volume compared to early 2nd instar fat body (Figure 5 A, B). During 3rd instar development, adipocytes undergo a partial cell detachment when dSPARC is overexpressed (Cg-Gal4<UAS-*dSPARC*::HA), whereas overexpression of dSPARC during early 2nd instar has no visible effect on adipocyte cell-cell adhesion (figure 5 B,D). The data indicate that CIVICs become necessary to promote adipocyte cell-cell adhesion as they reach volumes representative of late 2nd to early 3rd instar. Overexpression of dSPARC leads to a loss of Laminin in the CIVICs, but not the BM, around the partially detached adipocytes, supporting the previous conclusion that Collagen IV and Laminin glycoproteins associated with CIVICs have functions distinct from BMs (Figure 5 D).

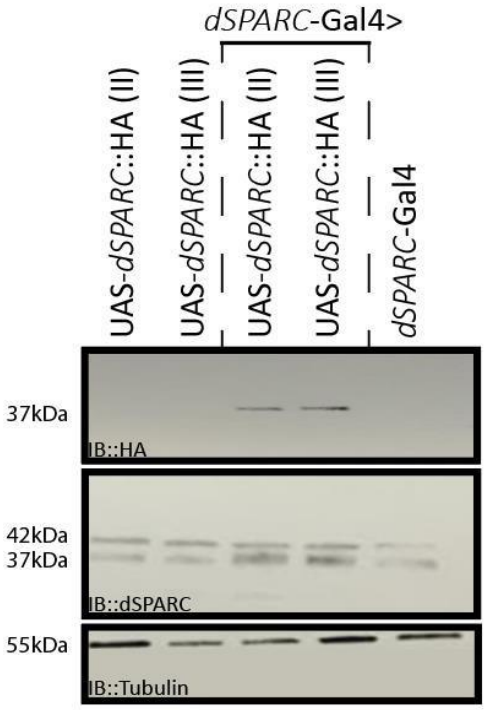


B. Fat Body

WT

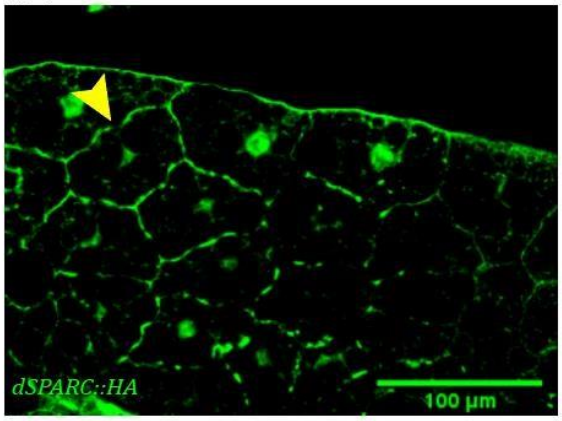


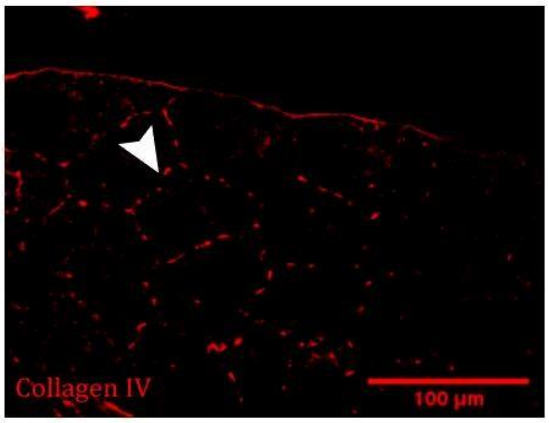


UAS-*dSPARC*::HA; *SPARC*-Gal4/ *SPARC*$^{1510D}$

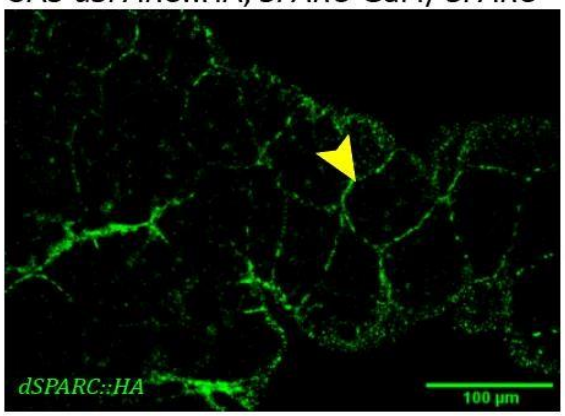


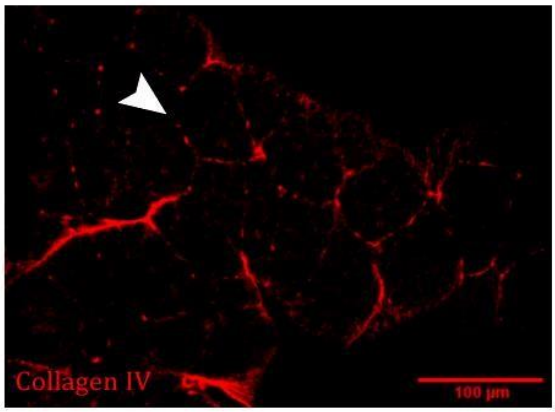

**Figure 4. Western blot and immunofluorescent analysis of dSPARC::HA.**

**A.** Western blot analysis of *dSPARC*::HA fly lysate from 3rd instar larvae immunoblotted with either anti-HA or anti-dSPARC antibodies. **A. Row 1.** Immunoblotting with anti-HA antibodies reveals a 37 kDa band corresponding to the expected molecular of weight dSPARC::HA. **Row 2.** Immunoblotting with anti-dSPARC antibody reveals an increase in band intensity when dSPARC is driven with *dSPARC*-Gal4 consistent with dSPARC overexpression. **B**. Wild-type 3rd instar fat body immunostaining with anti-dSPARC antibody reveals pericellular (yellow arrow) and nuclear-like localization. **B'.** Staining with anti-Cg25c reveals CIVICs (white arrow). Pericellular localization is also observed with anti-HA antibody **(C)** as well as CIVICs with anti-Cg25c **(C')** in larvae expressing dSPARC::HA in a $dSPARC^{10510D}$-mutant background.

A. WT 2nd to 3rd instar

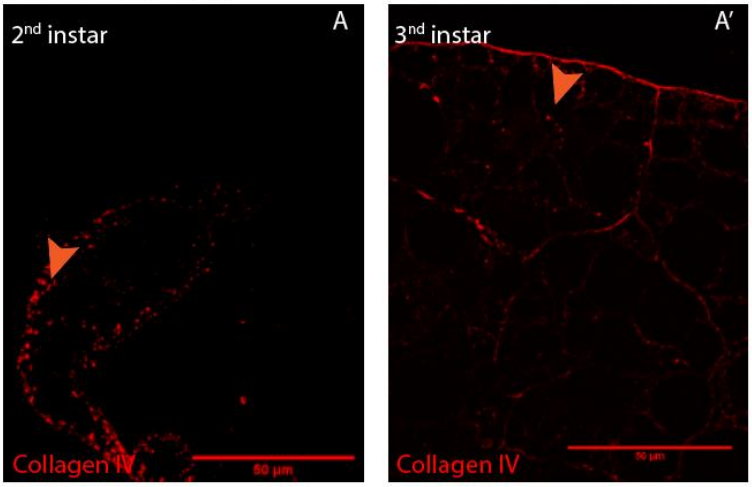


B. WT Adipocyte cell growth from 2nd to 3rd instar

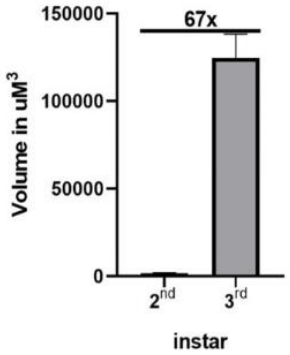


C. dSPARC-Gal4>SPARC::HA 2nd instar fat body

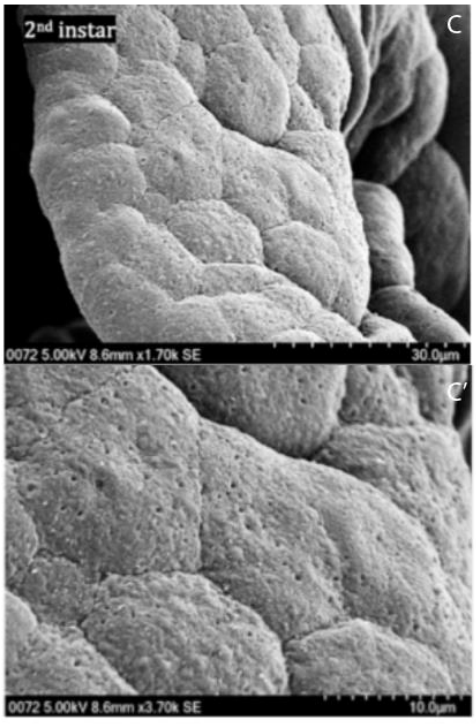


D. dSPARC-Gal4>SPARC::HA 3nd instar fat body

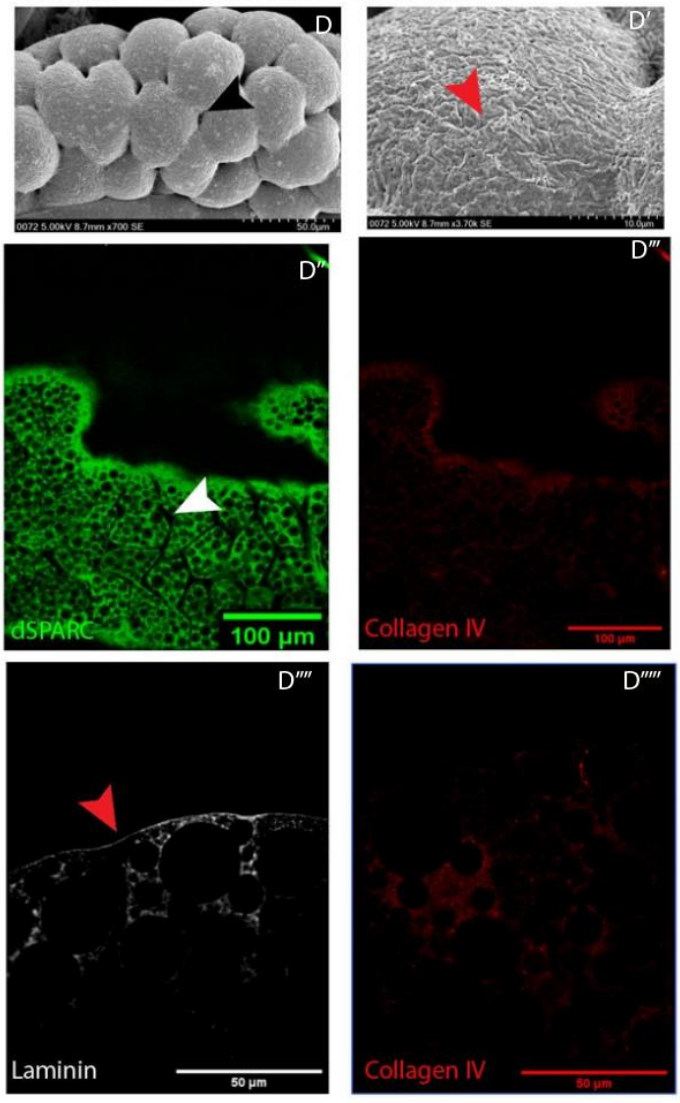

**Figure 5. Overexpression of dSPARC leads to a partial loss of adipocyte cell-cell adhesion in 3rd instar larva, but not 2nd instar larva.**

**A.** Wild-type fat body stained for Collagen IV reveal vesicular-like trafficking of Collagen IV (orange arrow)**,** with more vesicular-like structures in 2nd instar compared to 3rd instar larval (Scale bar = 50 µm). **B** Analysis of wild-type adipocytes reveals a 67-fold increase in cell volume between early 2nd instar (n=10) and wandering 3rd instar (n=10). **C-D**. Scanning electron microscopy of *dSPARC*-Gal4>UAS-*dSPARC*::HA at **(C)** 2nd instar does not show any major cell-cell detachment, while 3rd instar showed partial loss adipocyte cell-cell adhesion **(D-D')** (black arrow). Immunostaining with anti-dSPARC antibody is consistent with an overexpression of dSPARC **(D'')**. Immunostaining with anti-Cg25c reveals a loss of adipocyte Collagen IV in BM and an absence of CIVIC structures **(D'''')**, while Laminin is present in BM (red arrow)(**D''''**).

## 4.4 dSPARC Collagen-binding epitopes essential for proper intracellular and extracellular Collagen IV solubility

As previously noted, loss of dSPARC has been correlated with three phenotypes; 2nd instar larval lethality, fibrotic accumulation of BM components on adipocytes, and adipocyte cell rounding. I therefore sought to determine if phenotypic differences exist between the fat body of larvae arrested during 2nd instar as a result of an absence of dSPARC, compared to those that progressed to 3rd instar as a result of a KD of dSPARC. Heterozygous expression of a CRISPR *dSPARC*-mutant (*dSPARC*$^{1510D}$) engineered by Alexa Chiroan with a mutant allele (*dSPARC*-Gal4) expresses no SPARC protein (Chioran, 2017). As expected, the mutant background results in 2nd instar lethality, with a fibrotic accumulation of BM components surrounding the rounded adipocytes (figure 6B), hallmark features of 3rd instar fat body associated with dSPARC KD (Shahab *et al.*, 2015). However, the 2nd instar fat body adipocytes also displayed large intracellular vesicle rich in Collagen IV (figure 6B). Moreover, these vesicle-like structure do not appear to contain Laminin, suggesting that they may be selectively enriched in Collagen IV. The data raises the possibility that intracellular trafficking of Collagen IV is dependent on a direct interaction with dSPARC during 2nd instar larval development. Hence, to address this possibility a dSPARC transgenic line containing mutations in amino acids essential for SPARC Collagen binding (UAS-*dSPARC*$^{mCBD}$::HA) was engineered.

My immunofluorescence data suggests that higher levels of intracellular Collagen IV appear to be present in 2nd instar compared to 3rd instar fat body (Figure 5A), raising the possibility that proper levels of dSPARC and direct interaction with Collagen IV is required for Collagen IV secretion during high Collagen IV production such as in 2nd instar fat body development. Transgenic expression of UAS-*dSPARC*$^{mCBD}$::HA with *dSPARC*-Gal4 failed to rescue 2nd instar larval lethality (Figure 6 D). Furthermore, immunofluorescent analysis of 2nd instar larvae revealed an accumulation of Collagen IV in large intracellular vesicle-like structures rich in Collagen IV, similar to that observed in 2nd instar of the *dSPARC*$^{1510D}$ -mutant (Figure 6C). Therefore, a direct interaction between dSPARC and Collagen IV appears necessary to prevent intracellular accumulation of Collagen IV. Interestingly, *dSPARC*$^{mCBD}$::HA also co-localized with Collagen IV in this vesicle-like structures. Hence, their intracellular recruitment and co-localization in this large vesicle-like structures appears to be independent of direct association with each other. Additionally, the lack of UAS-*dSPARC*$^{mCBD}$::HA in the BM indicates that a direct

interaction with Collagen IV is also essential for dSPARC incorporation in 2nd instar fat body BM. An alternative possibility is that loss of dSPARC may promote Collagen IV endocytosis, thereby increasing the amount of intracellular Collagen IV. This is unlikely as it would not explain the vesicular like entrapment of *dSPARC*$^{mCBD}$::HA, as it is not retained in the BM. Therefore, wild-type dSPARC appears essential for the extracellular secretion of Collagen IV in 2nd instar fat body. Unexpectedly, a *dSPARC*$^{1510D}$/*dSPARC*-Gal4> UAS-*dSPARC*$^{mCBD}$::HA displayed lower Collagen IV immunofluorescence in the BM and decrease of adipocyte rounding than the *dSPARC*$^{1510D}$/*dSPARC*-Gal4 despite both resulting in 2nd instar larval lethality (Figure 6B,C). Thus, the data indicate that *dSPARC*$^{mCBD}$::HA is able to partially rescue a Collagen IV fibrosis in BM despite a substantial decrease in affinity for Collagen IV.

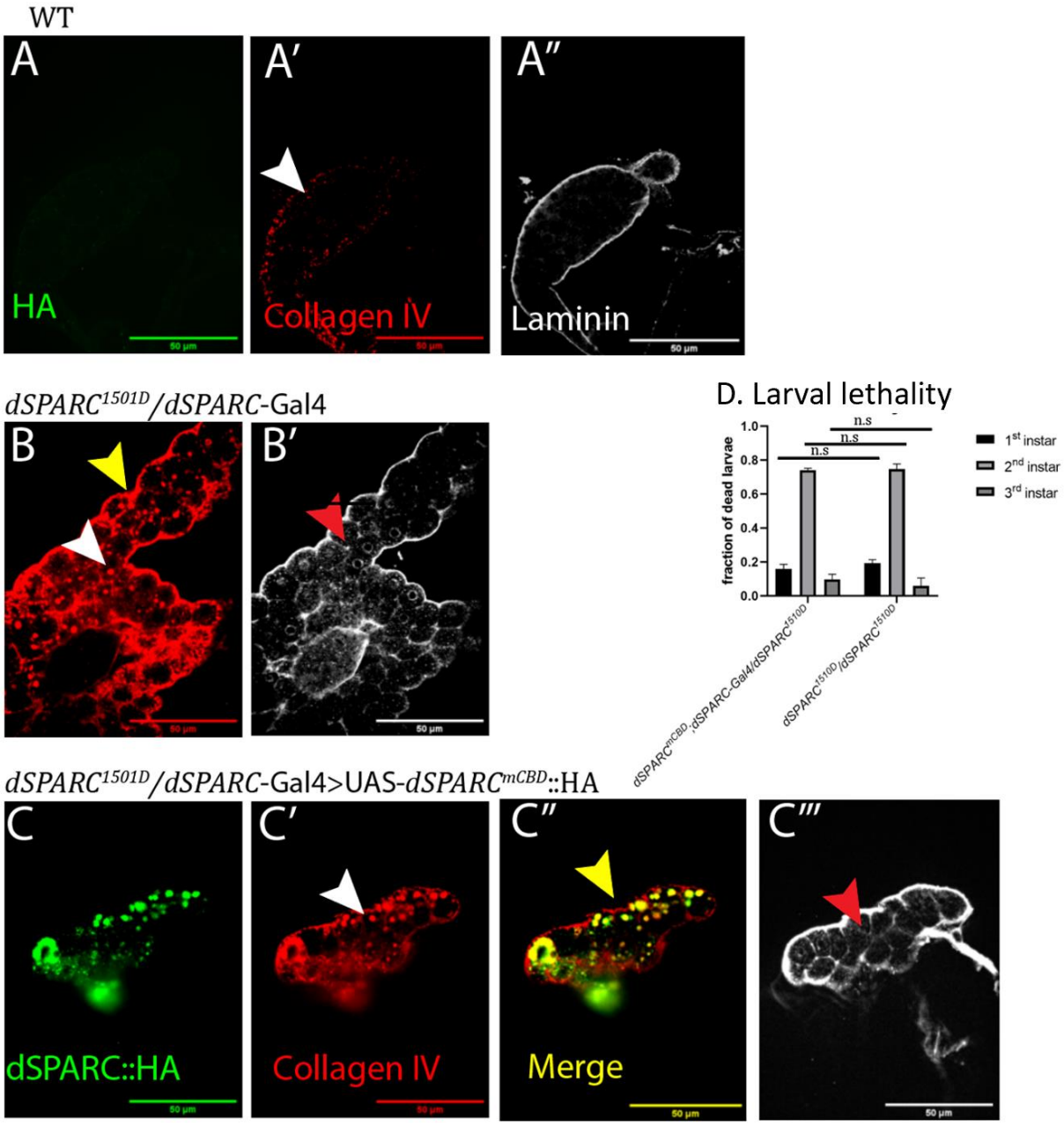
WT
A
HA
A′
Collagen IV
A″
Laminin
50 µm
dSPARC1501D/dSPARC-Gal4
B
B′
D. Larval lethality
fraction of dead larvae
1.0
0.8
0.6
0.4
0.2
0.0
n.s
n.s
n.s
1st instar
2nd instar
3rd instar
dSPARCmCBD,dSPARC-Gal4/dSPARC1510D
dSPARC1510D/dSPARC1510D
dSPARC1501D/dSPARC-Gal4>UAS-dSPARCmCBD::HA
C
dSPARC::HA
C′
Collagen IV
C″
Merge
C‴

**Figure 6. Transgenic expression of *dSPARC*$^{mCBD}$::HA in a dSPARC-mutant background reveals intracellular entrapment and premature formation of CIVICs in 2nd instar fat body adipocytes.**

**A'.** 2$^{nd}$ instar wild-type staining with anti-Cg25c antibody reveals small intracellular Collagen rich vesicles (white arrow) and an absence of CIVIC structures. **B.** Staining of *dSPARC*$^{1051D}$-mutant with anti-Cg25c antibody shows an increase in the size of Collagen IV-rich intracellular vesicle-like structures (white arrow) with premature CIVICs, (red arrow) and accumulations of extracellular Collagen IV (yellow arrow). **C.** *dSPARC*$^{1051D}$*/dSPARC*-Gal4>*dSPARC*$^{mCBD}$::HA, also exhibited large intracellular vesicles containing *dSPARC*$^{mCBD}$::HA and Collagen IV (white arrow), with extracellular accumulation of Collagen IV (yellow arrow) and premature formation of CIVICs (red arrow). **D.** Larval lethality assay for dSPARC-Gal4/*dSPARC*$^{1510D}$ and *dSPARC*$^{1510D}$/dSPARC-gal4>*dSPARC*$^{mCBD}$::HA shows lethality occurs at 2$^{nd}$ instar, with no statistical significance between the two genotypes ($p>0.05$).

To circumvent 2nd instar lethality and assess the impact of *dSPARC*$^{mCBD}$::HA on 3rd instar fat body BM homeostasis, dSPARC$^{mCBD}$::HA was driven with dSPARC-Gal4 in a wild-type background. The transgenic expression of *dSPARC*$^{mCBD}$::HA showed similar pericellular distribution at adipocytes as endogenous dSPARC in wild-type larvae (Figure 7). In contrast to 2nd instar fat body where *dSPARC*$^{mCBD}$::HA is not retained pericellularly (Figure 6C). Thus, the data indicate that localization of dSPARC maybe in part independent of a direct interaction with Collagen IV. However transgenic expression of *dSPARC*$^{mCBD}$::HA had no impact on the distribution of Collagen IV in BM (Figure 7), in contrast to the transgenic expression of *dSPARC*::HA in a WT background which led to a decrease in Collagen IV retention in BM (Figure 5D). The data indicate that the Collagen binding epitopes of dSPARC are critical for Collagen IV solubility, but not required for 3rd instar dSPARC pericellular localization. It remains possible that while dSPARC$^{mCBD}$::HA is unable to bind Collagen IV, while its retention in BM is mediated by other protein(s) that are localized to the pericellular domain of adipocytes. To test this hypothesis I determined if *dSPARC*$^{mCBD}$::HA diffuses and becomes incorporated on a BM that is assembled unto the surface of the wing imaginal discs similar to adipocyte produced Collagen IV and Perelecan, which would have all BM core components, but not necessarily the exact same protein complement of the pericellular adipocyte microenvironment.

As shown in Figure 8A/B, fat body-derived *dSPARC*::HA diffuses to and associates with the wing imaginal disc BM. In contrast, *dSPARC*$^{mCBD}$::HA driven with *dSPARC*-Gal4, fails to localize in the BM of the wing imaginal disc (Figure 8C), indicating that dSPARC association with the wing imaginal BM is dependent on dSPARC having an affinity for Collagen IV. As dSPARC is also expressed by the wing imaginal disc, it is possible that dSPARC localized to the wing imaginal disc, is partially derived from the wing imaginal disc epithelium. To explore this possibility, the expression of dSPARC was knocked down in the wing imaginal disc to determine if dSPARC is exclusively derived from the fat body.

## 4.5 Fat body and wing-derived dSPARC have distinct distribution

To differentiate between these two possibilities, dSPARC expression was KD in the wing imaginal discs using a dSPARC RNAi driven by engrailed-Gal4, which is expressed in the posterior side of the imaginal disc of 3rd instar larval (*en*-Gal 4>UAS-SPARC$^{RNAi\text{-}16678}$). KD of dSPARC in the wing imaginal discs resulted in a similar immunostaining of dSPARC and

Collagen IV as in control discs (figure 9). Thus, the data indicate that dSPARC in the BM is predominantly derived from the fat body adipocytes. This raises the question as to why the wing imaginal disc expresses dSPARC and whether this source of dSPARC has any impact on fat body BM assembly and stability. Surprisingly, *dSPARC*::HA driven by *en*-Gal4 in the wing imaginal disc, does not associate to the wing imaginal disc BM. Moreover, the levels of Collagen IV at the wing imaginal disc BM were unaffected despite the expression of *dSPARC*::HA and endogenous dSPARC by the wing imaginal discs. This contrasts with the decrease of Collagen IV immunostaining observed in fat body BM when dSPARC is overexpressed by the adipocytes (Figure 5D). Moreover, the wing imaginal disc-derived *dSPARC*::HA diffused to the fat body, but does not concentrated in fat body BM. Instead it showed a punctate distribution at the adipocyte cell border that partially overlaps but is distinct from Collagen IV distribution (Figure 10A). The collective data raises the possibility that the wing imaginal disc-derived dSPARC undergoes a post-translational modification that is distinct from fat body-derived dSPARC, allowing for Collagen IV independent localization. Lending support to a potential identification of a novel dSPARC isoform expressed by the wing imaginal discs, both wing imaginal disc-derived *dSPARC*::HA and $dSPARC^{mCBD}$::HA exhibit a similar distribution profile in the fat body (Figure 10B).

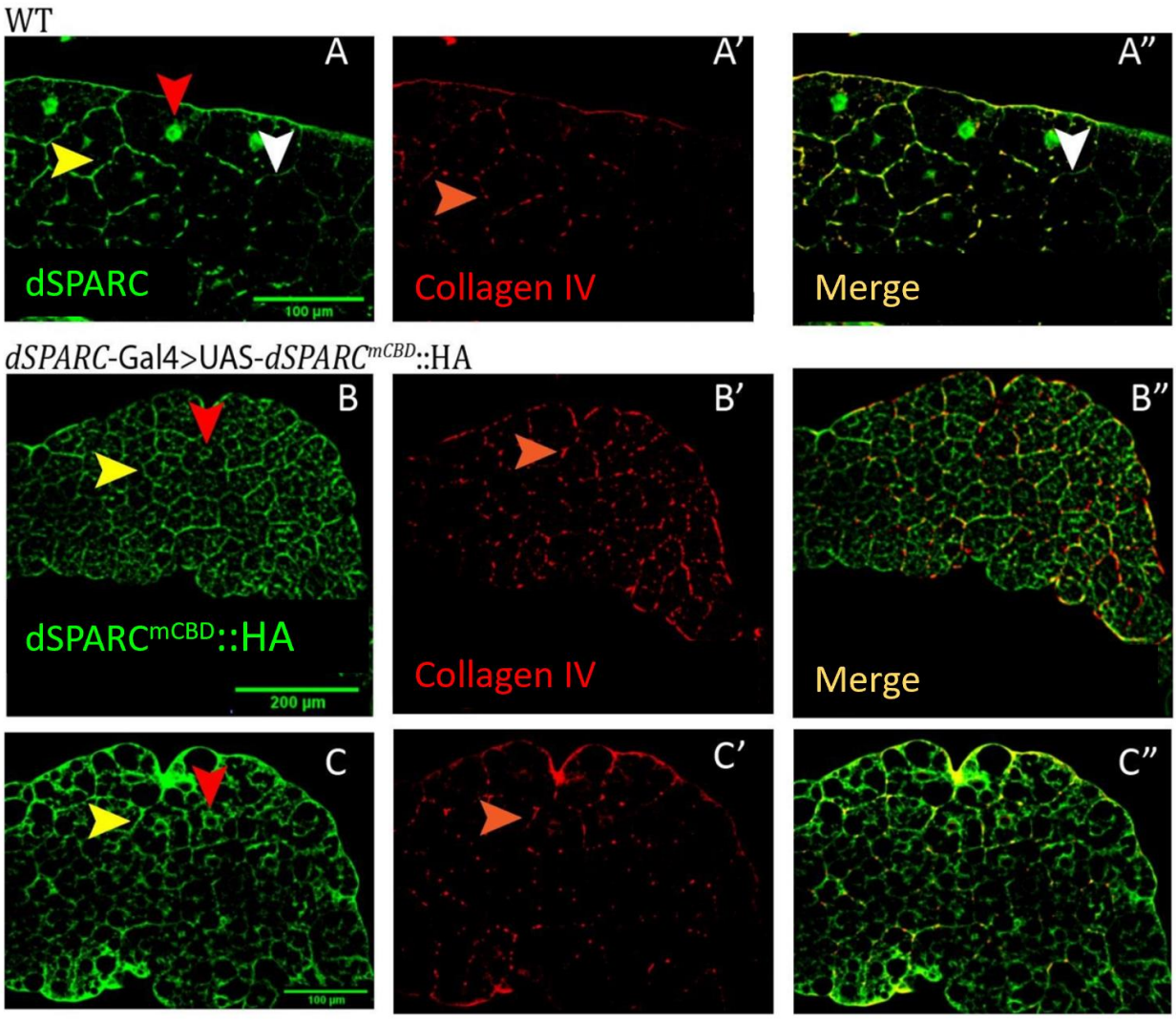
WT
A
A'
A"
dSPARC
100 µm
Collagen IV
Merge
dSPARC-Gal4>UAS-dSPARCmCBD::HA
B
B'
B"
dSPARCmCBD::HA
200 µm
Collagen IV
Merge
C
C'
C"
100 µm

**Figure 7. Immunolocalization of dSPARC and Collagen IV in wild-type and dSPARC$^{mCBD}$::HA 3$^{rd}$ instar larval fat body.**

**A**. Wild-type immunofluorescence analysis of 3$^{rd}$ instar fat body with anti-dSPARC antibody reveals cell border (yellow arrow) and nuclear-like localization (red arrow). **A'.** Collagen IV staining shows CIVICs staining (orange arrow). **A''.** Merged images of dSPARC and Collagen IV staining show overlapping and non-overlapping regions (white arrow). *dSPARC*-Gal4>UAS-*dSPARC$^{mCBD}$*::HA in a wild-type background also shows cell border localization **(B)** and nuclear-like staining (yellow and red arrow)**.**

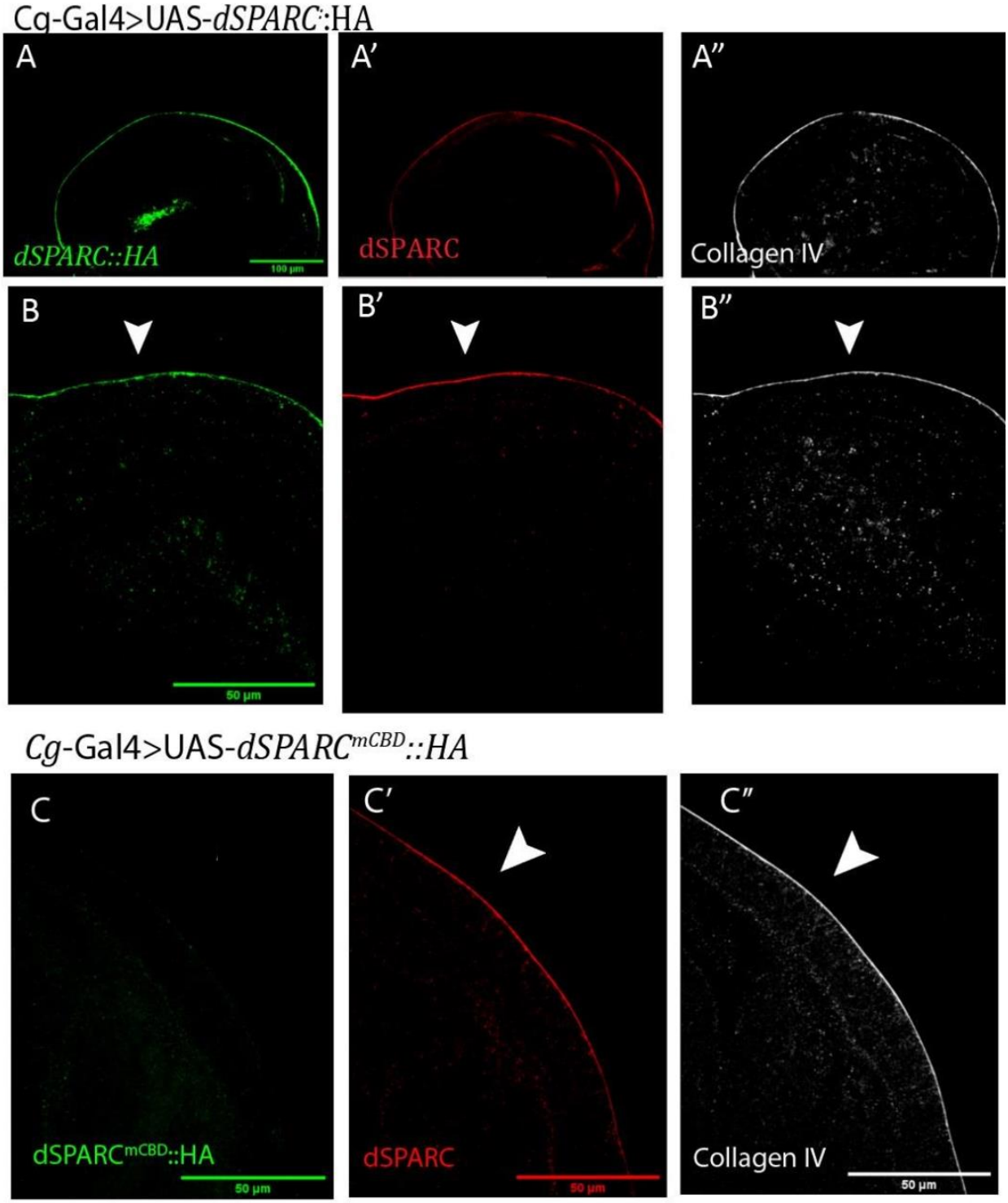
Cg-Gal4>UAS-dSPARC:HA
A
A'
A"
dSPARC::HA
100 µm
dSPARC
Collagen IV
B
B'
B"
50 µm
Cg-Gal4>UAS-dSPARC^mCBD::HA
C
C'
C"
dSPARC^mCBD::HA
50 µm
dSPARC
50 µm
Collagen IV
50 µm

**Figure 8. Immunolocalization of fat body-derived *dSPARC*::HA and *dSPARC*$^{mCBD}$::HA in 3rd instar wing imaginal disc BM.**

**A-B.** Immunostaining with anti-HA antibody of Cg-Gal4>*dSPARC::*HA in a wild-type background showed *dSPARC*::HA localization in the BM of the wing imaginal discs (white arrow), mirroring the immunostaining of anti-dSPARC and anti-Cg25c antibodies (**A'-A").** In contrast, Cg-Gal4>*dSPARC*$^{mCBD}$*::*HA in a wild-type background does not localize to the BM of the wing imaginal discs, when immunostaining with anti-HA antibody **(C)**.

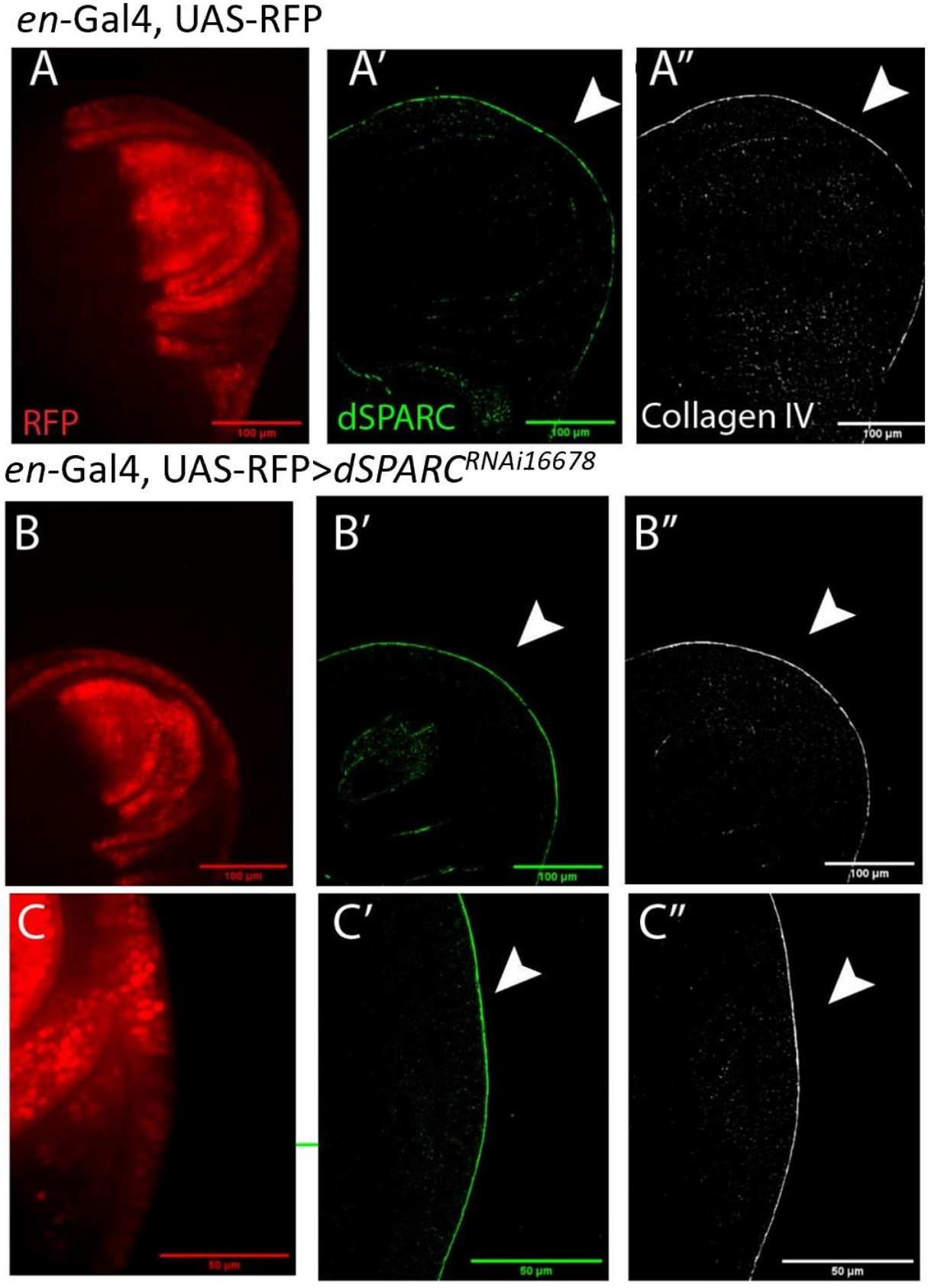
en-Gal4, UAS-RFP
A
A′
A″
RFP
dSPARC
Collagen IV
100 µm
en-Gal4, UAS-RFP>dSPARCRNAi16678
B
B′
B″
C
C′
C″
50 µm

**Figure 9. Knockdown of wing imaginal disc-derived dSPARC has no impact on dSPARC or Collagen IV levels in wing imaginal disc BMs.**

**A**. Immunostaining with anti-dSPARC and anti-Cg25c antibodies shows that expression of Gal4 in the posterior section (*en*-Gal4, UAS-RFP) of the imaginal discs **(A)** does not affect BM localization of dSPARC **(A')** or Collagen IV **(A")** as indicated by the white arrow. Likewise, removal of dSPARC expression from the posterior section of the wing imaginal disc (En-Gal4, UAS-RFP>dSPARC$^{RNAi16678}$) does not affect **(B')** dSPARC or **(B")** Collagen IV levels in the wing imaginal disc BM (white arrow). **C.** Higher magnification of images in section of B.

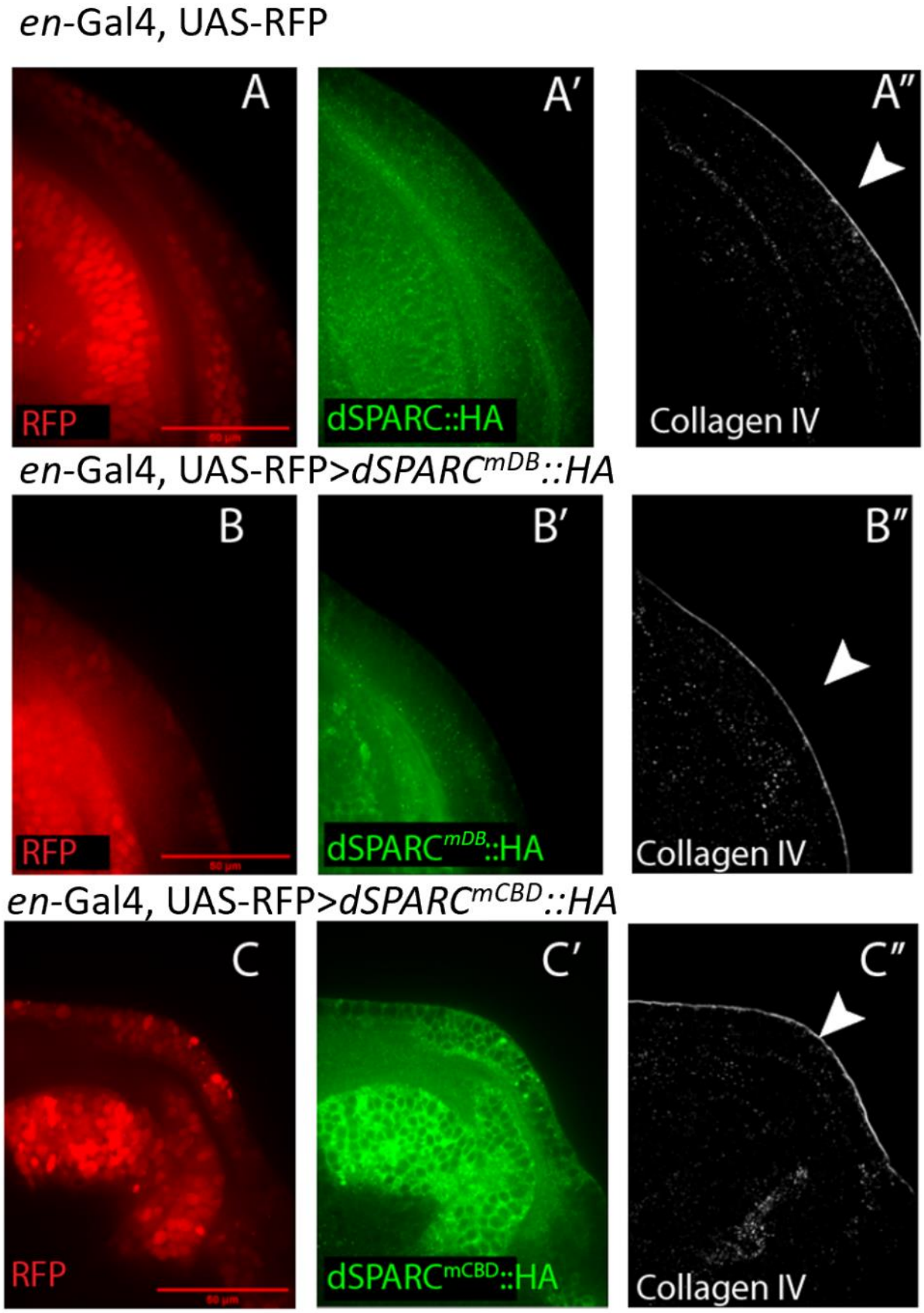
en-Gal4, UAS-RFP
A
A′
A″
RFP
dSPARC::HA
Collagen IV
en-Gal4, UAS-RFP>dSPARCmDB::HA
B
B′
B″
RFP
dSPARCmDB::HA
Collagen IV
en-Gal4, UAS-RFP>dSPARCmCBD::HA
C
C′
C″
RFP
dSPARCmCBD::HA
Collagen IV

**Figure 10. Wing imaginal disc-derived dSPARC::HA, dSPARC$^{mCBD}$::HA, and dSPARC$^{mDB}$::HA do not localize in the wing imaginal discs BM.**

Wing imaginal discs expressing **(A)** dSPARC::HA, **(B)** dSPARC$^{mDB}$::HA or **(C)** dSPARC$^{mCBD}$::HA in the posterior compartment under *en*-Gal4. dSPARC from all three constructs did not localize to the wing imaginal disc BM when immunostaining with anti-HA antibody **(A'-C')**. Additionally, Collagen IV is still present in the BM of all three constructs shown with anti-Cg25c antibody (white arrow) **(A"-C")**

*en*-Gal4, UAS-RFP>*dSPARC::HA*

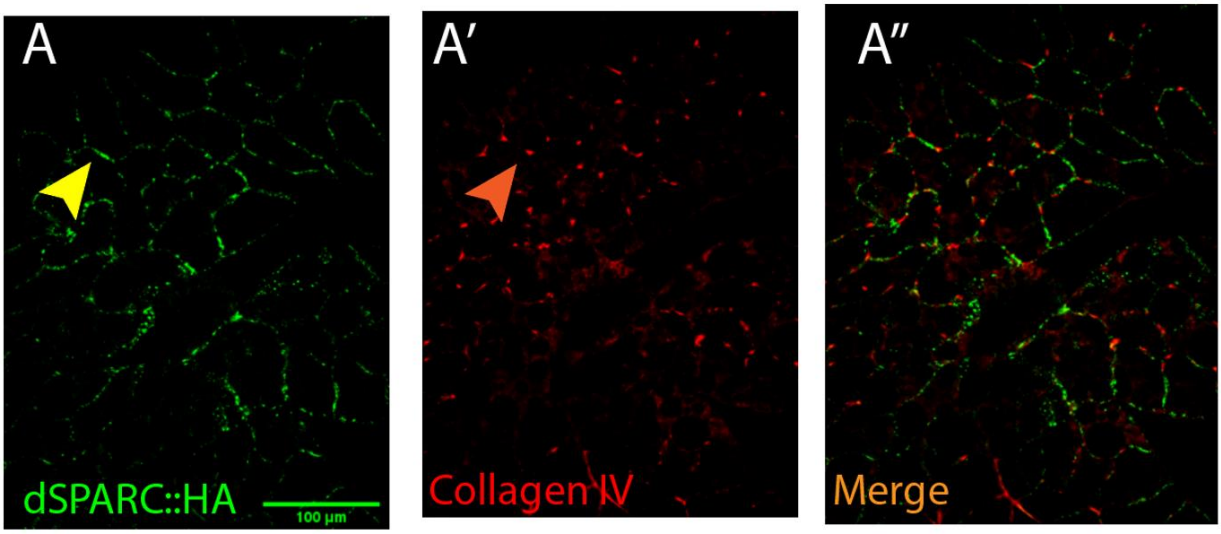


*en*-Gal4, UAS-RFP>*dSPARC$^{mCBD}$::HA*

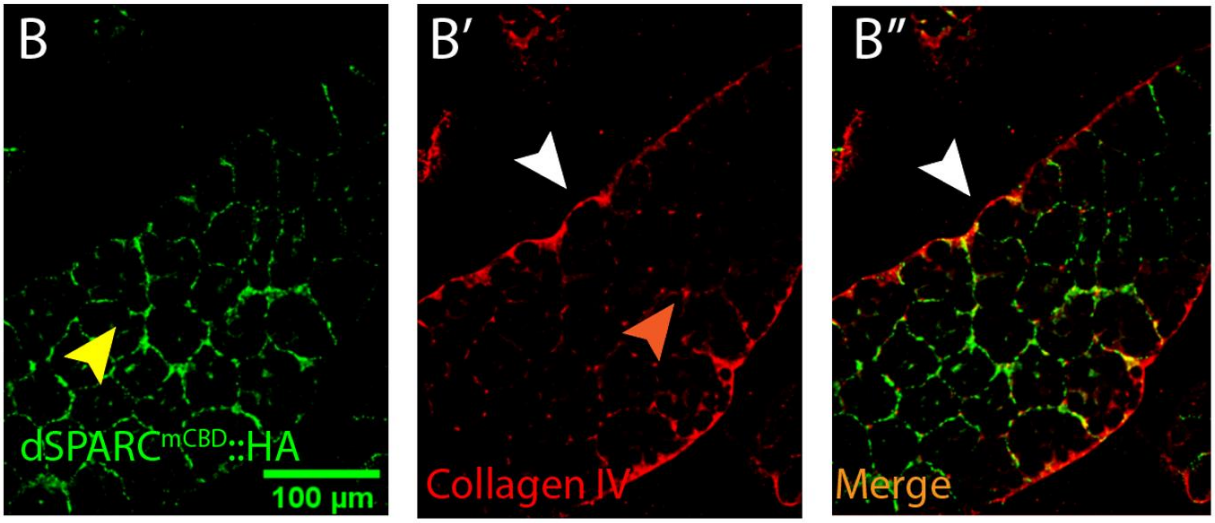

**Figure 11. Wing imaginal disc derived *dSPARC*::HA, and *dSPARC*$^{mCBD}$::HA, diffuse and localize to the fat body adipocytes cell borders but not their BMs.**

Immunohistochemistry of third instar fat body expressing **(A)** *dSPARC*::HA **(B)** *dSPARC*$^{mCBD}$::HA under *en*-Gal4, in the posterior compartment of the 3$^{rd}$ instar larval discs. **A-B** Immunostaining with anti-HA antibody for both constructs reveal pericellular fat body adipocyte localization of the wing imaginal disc derived-dSPARC (yellow arrow). Additionally, both constructs displayed CIVICs (orange arrow) when stained with anti-Cg25c antibody (**A'-B'). A"-B"** represent merged images of A with A' and B with B' respectively.

## 4.6 Loss of disulfide bridge of dSPARC Ef-hand2 results in an aberrant accumulation of BM components disrupted with numerous BM pores

I*n vitro* biochemical studies have reported that the highly conserved disulfide bridge of EF-hand2 enhances the affinity of SPARC for Collagen IV (Pottgiesser *et al.*, 1994). My *in vivo* data indicate that driving expression of *dSPARC*$^{mDB}$::HA rescues *dSPARC*-mutant flies to adulthood. Unexpectedly, despite the rescue to adulthood, 3$^{rd}$ instar fat body adipocytes were rounded with fibrotic-like accumulation of Collagen IV in BM (figure 12). Moreover, a dramatic increase in the number of circular pores with elevated borders are observed in the BM of UAS-*dSPARC*$^{mDB}$::HA relative to wild-type larvae (figure 13). The collective morphological changes phenocopy previous data obtained with RNAi knock down of dSPARC (Figure 12-13). In contrast to dSPARC$^{RNAi\text{-}16678}$ larvae, which showed no Collagen IV in the wing imaginal discs (Pastor-Pareja and Xu, 2011), *dSPARC*$^{mBD}$::HA expression driven with dSPARC-Gal4 in a *dSPARC*-mutant background has Collagen IV at higher levels in the BM of wing imaginal discs compared to control wild type larval. The combined data indicate that larval lethality resulting from the loss of dSPARC protein is not simply due to the loss of fat body BM homeostasis. In support of this hypothesis, temperature-sensitive knockdown of dSPARC during embryogenesis and subsequent reactivation of expression during 1$^{st}$ instar fails to rescue larval lethality.

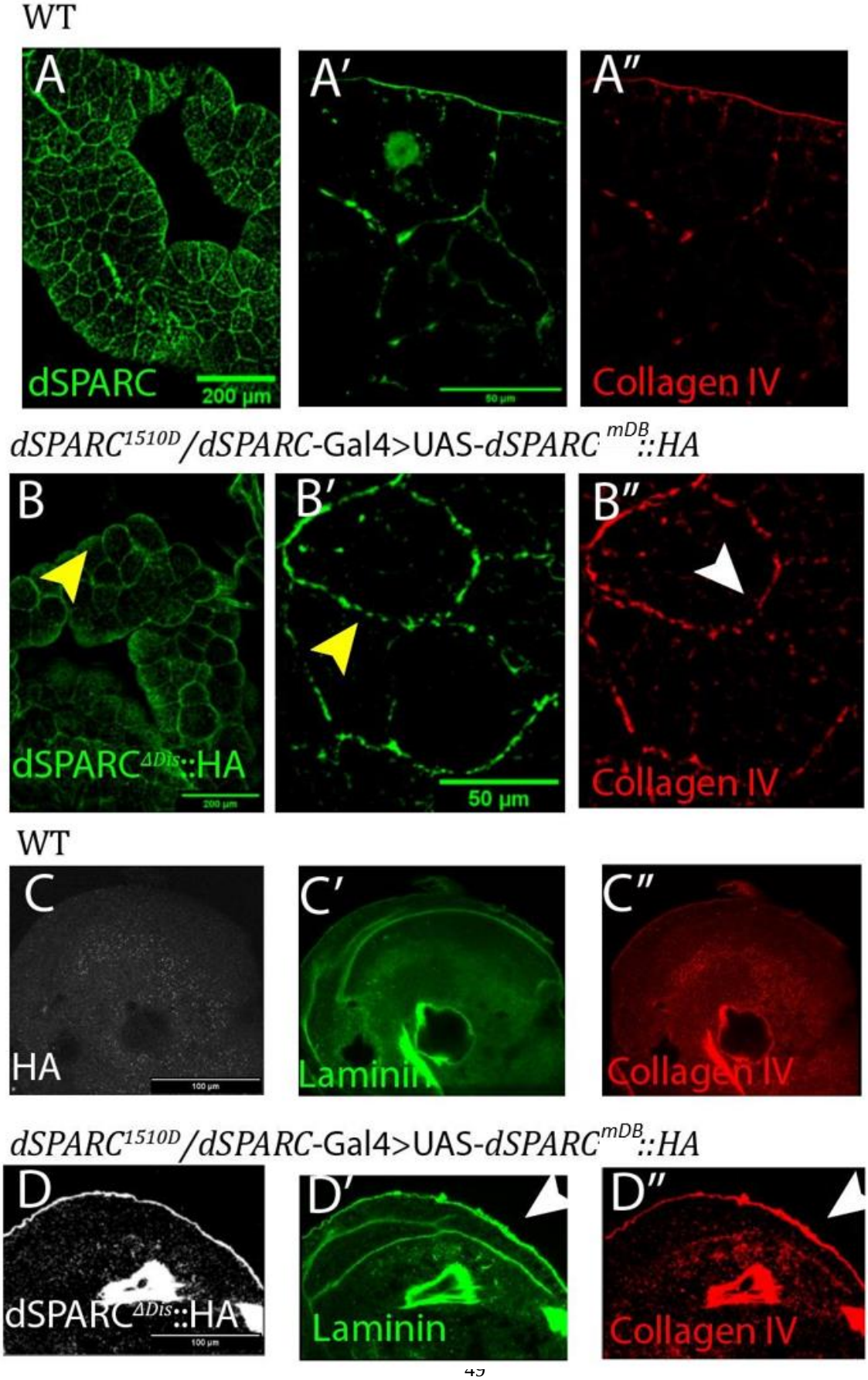
WT
A
dSPARC
200 µm
A′
A″
Collagen IV
dSPARC1510D/dSPARC-Gal4>UAS-dSPARC mDB::HA
B
dSPARCΔDis::HA
B′
50 µm
B″
Collagen IV
WT
C
HA
C′
Laminin
C″
Collagen IV
dSPARC1510D/dSPARC-Gal4>UAS-dSPARCmDB::HA
D
dSPARCΔDis::HA
D′
Laminin
D″
Collagen IV

**Figure 12. Transgenic expression of *dSPARC*$^{mDB}$::HA in a *dSPARC*-mutant background shows adipocyte cell rounding and BM accumulation at the fat body and wing imaginal disc.**

**A.** Immunostaining of wild-type fat body, with dSPARC antibody reveals pericellular localization and nuclear-like staining **(A'),** with anti-Cg25c antibody revealing CIVICs and BM **(A"). B.** Immunostaining with either dSPARC or Cg25c of *dSPARC*$^{10510D}$*/dSPARC*-Gal4>*dSPARC*$^{mDB}$::HA exhibits cell rounding (yellow arrow) and accumulation of dSPARC and Collagen IV (white arrow). **C**. Wild-type wing imaginal disc immunostaining with anti-laminin and anti-Cg antibodies revealed staining in the BM of the wing imaginal disc. **D.** dSPARC-Gal4>*dSPARC*$^{mDB}$::HA in a *dSPARC*$^{10510D}$-mutant background displayed an accumulation of BM components Laminin and Collagen IV (white arrow) at BM of the wing imaginal disc compared to wild-type.

WT

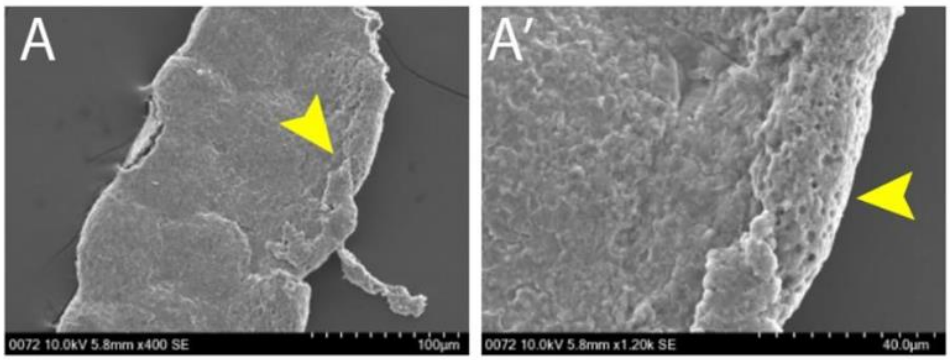


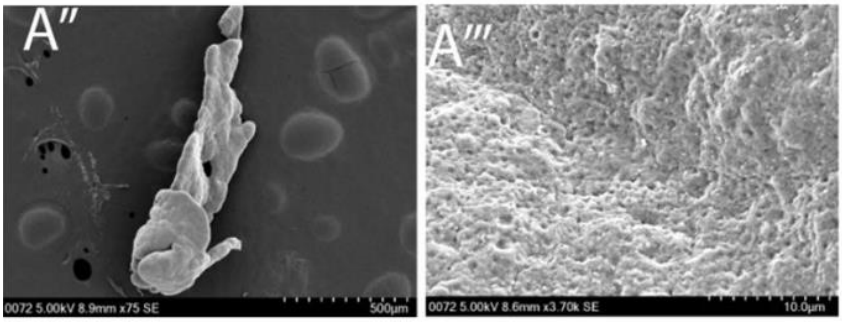


*dSPARC*$^{1501D}$/*dSPARC*-Gal4 > UAS-*dSPARC*$^{mDB}$::HA

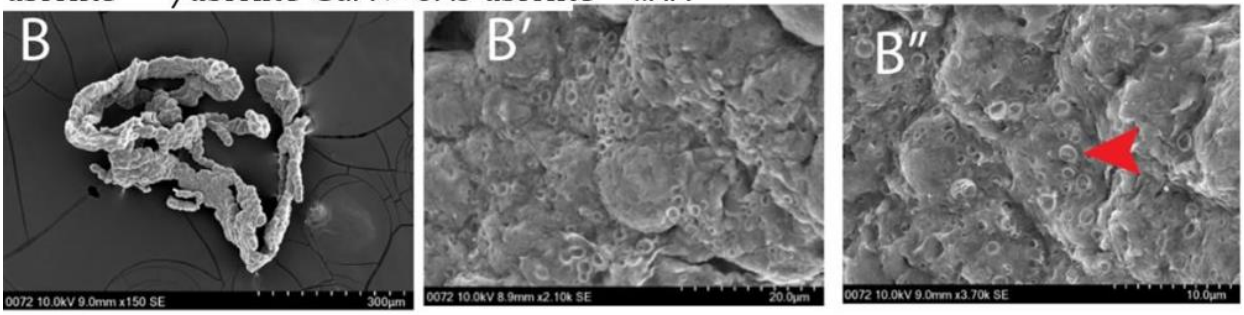


dSPARC-Gal4>UAS-dSPARC$^{RNAi-16678}$

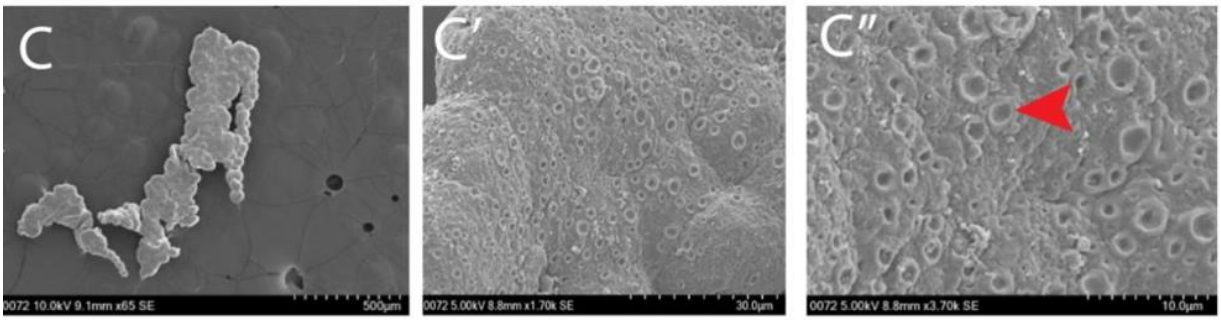

**Figure 13. Scanning electron microscopy of fat body from wild type, *dSPARC*$^{mDB}$::HA and dSPARC$^{RNAi-16678}$.**

**A-A'**. Scanning electron microscopy of 3$^{rd}$ instar wild-type fat body reveals a partially torn BM. Small pores are precent on the surface of the BM (yellow arrow) and not the cell surface. **(A'A").** Expression of *dSPARC*$^{mDB}$::HA in a *dSPARC* mutant or *dSPARC*$^{RNAi-16678}$ driven with *dSPARC*-Gal4 both yield an increase in pore size and the formation of lips surrounding the pore borders as indicated by the red arrows **(B"-C")**.

## 4.7 Cytoplasmic translation of *dSPARC*$^{\Delta SP}$::HA is associated with an increased molecular weight and localization to the cell border of larval adipocytes

Studies with vertebrate organisms have long eluted to potential intracellular functions for SPARC, mediated by an intracellular isoform referred as iSPARC. Hence a dSPARC construct lacking the signal peptide (UAS-*dSPARC*$^{\Delta SP}$::HA) was engineered to restrict dSPARC translation to the cytoplasm and prevent secretion through the secretory pathway. I sought to confirm in a wild-type background that *dSPARC*$^{\Delta SP}$::HA is not degraded and has a lower molecular weight than endogenous dSPARC due to an absence of glycosylation. As a control, transgenic expression of dSPARC::HA in a WT background was analysed by western blot analysis. As expected, an intense band of 37 kDa is evident with anti-HA antibody, corresponding to the expected molecular weight of dSPARC, in addition to an unknown minor band of 67 kDa (Figure 14). Unexpectedly, transgenic expression of *dSPARC*$^{\Delta SP}$::HA yielded only a single intense band also of 67 kDa with the HA antibody. Thus, the data indicate that cytosolic translation of dSPARC results in a protein product with of molecular weight approximately twice the molecular weight of endogenous dSPARC, suggesting that iSPARC undergoes an unknown post-translational modification.

Transgenic expression of *dSPARC*$^{\Delta SP}$::HA with *dSPARC*-Gal4 in a wild-type background, indicates that the 67 kDa protein is concentrated in a punctate manner at the adipocyte cell cortex (Figure 15). Cytosolic *dSPARC*$^{\Delta SP}$::HA has no impact on Collagen IV deposition in 3$^{rd}$ instar larval fat body adipocytes BM and CIVICs. However, expression of *dSPARC*$^{\Delta SP}$::HA driven by *dSPARC*-Gal4 failed to rescue *dSPARC* mutant flies *(dSPARC*$^{1510D}$*/dSPARC*-Gal4). Hence, it is important to first determine the nature of the post-translational modification for iSPARC before attempting to unmask potential intracellular function(s).

### Transgenic expression of *hSPARC* fails to rescue a *dSPARC*-mutant background

The Collagen binding domain and disulfide bridge EF hand2 of SPARC are highly conserved from cnidarians to vertebrates, suggesting an evolutionary conservation of SPARC function in BM assembly and stability. I therefore wanted to explore if a human SPARC fusion construct could rescue the loss of dSPARC. As a first step, I investigated if transgenic expression of a

hSPARC $^{hSP}$::HA (human signal peptide) could yielded a protein that is not degraded in *Drosophila*. Protein lysate derived from transgenic flies coding *hSPARC*$^{hSP}$::HA in a wild-type background and probed with an anti-HA antibody, results in a prominent band of 67 kDA and a minor 37 kDA band (Figure 14). The intense 67 kDa band indicates that the majority of *hSPARC*$^{hSP}$ is potentially translated in the cytoplasm and post-translationally modified in a manner similar to *dSPARC*$^{\Delta SP}$::HA. Moreover immunostanining indicates *dSPARC*$^{hSP}$::HA is not observed in fat body BMs (Figure 16). Additionally, transgenic expression of of *dSPARC*$^{hSP}$::HA is unable to rescue loss of dSPARC (summary in Figure 17). A previous study reported that human proteins are not efficiently secreted unless the human signal peptide is substituted for an insect signal peptide (Futatsumori-Sugai and Tsumoto, 2010). Hence, expressing of *dSPARC*$^{hSP}$::HA mRNA may not be effectively targeted to the ER for translation, but rather translated in the cytoplasm which could account for a lack of a rescue. To test this hypothesis, a hSPARC construct was engineered with a *Drosophila* signal peptide (*hSPARC*$^{dSP}$). Western blot analysis with anti-hSPARC antibody revealed a single band at 37 kDa and a weaker band at 42 kDa (Figure 14). The 37 kDa band corresponds to the expected molecular weight of secreted dSPARC when translated in the ER. The identity of the 42 kDa, while consistenly observed, remains to be determined. As with *hSPARC*$^{hSP}$::HA, *hSPARC*$^{dSP}$ failed to rescue a loss of dSPARC. Moreover, the cellular distribution of *hSPARC*$^{dSP}$ (Figure 16) is similar to that of *dSPARC*$^{mCDB}$::HA (Figure 5) both of which have no convincing evidence of BM association. While hSPARC$^{dSP}$contains both highly conseved Collagen binding epitopes and the EF-hand2 disulfide bridge, it is unable to rescue loss of dSPARC and associated with BM for unknown reason(s).

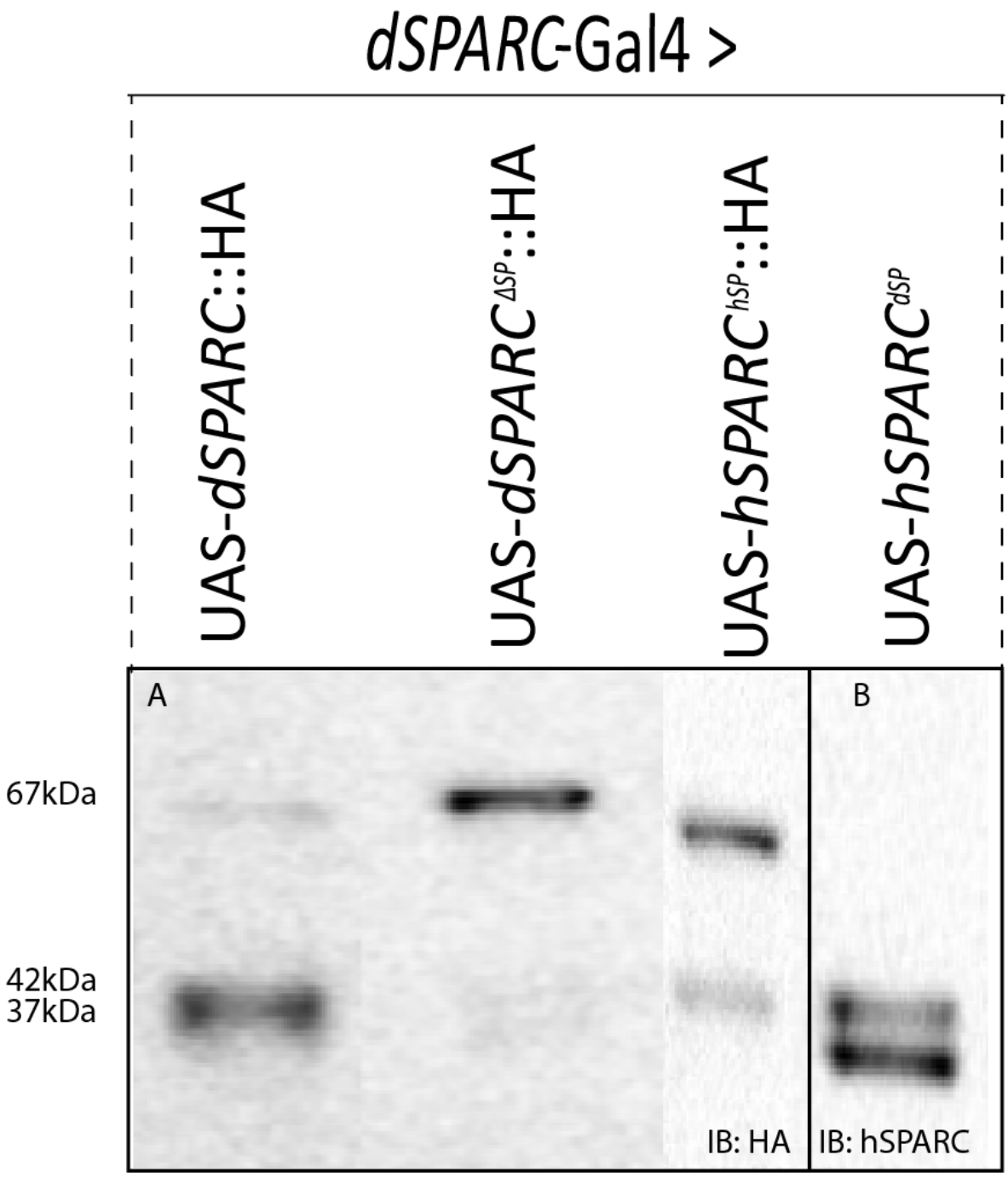
dSPARC-Gal4 >
UAS-dSPARC::HA
UAS-dSPARC^ΔSP::HA
UAS-hSPARC^hSP::HA
UAS-hSPARC^dSP
A
B
67kDa
42kDa
37kDa
IB: HA
IB: hSPARC

**Figure 14. Western blot of *dSPARC*::HA constructs driven with *dSPARC*-Gal4.**

**A.** Western blot analysis of protein derived from *dSPARC*::HA or $dSPARC^{\Delta SP}$::HA driven with *dSPARC*-Gal4 immunoblotted with anti-HA antibody**. Lane 1.** Measurement of *dSPARC::HA* shows an intense band at 37 kDa, with a minor band at 67 kDa. **Lane 2.** In contrast $dSPARC^{\Delta SP}$, reveals a single band at 67 kDa. **Lane 3.** $hSPARC^{hSP}$::HA reveals a weak 37 kDa band, which correlates with the expected molecular weight of ER translated dSPARC and an intense 67 kDa band matching the hypothesize molecular weight of the cytosolically translated dSPARC. **B. Lane 1.** Analysis of *dSPARC*-Gal4>$hSPARC^{dSP}$ with anti-hSPARC antibody shows two bands; a 37 kDA band corresponding to the expected molecular weight for the secreted isoform of dSPARC, and an unidentified 42 kDa band.

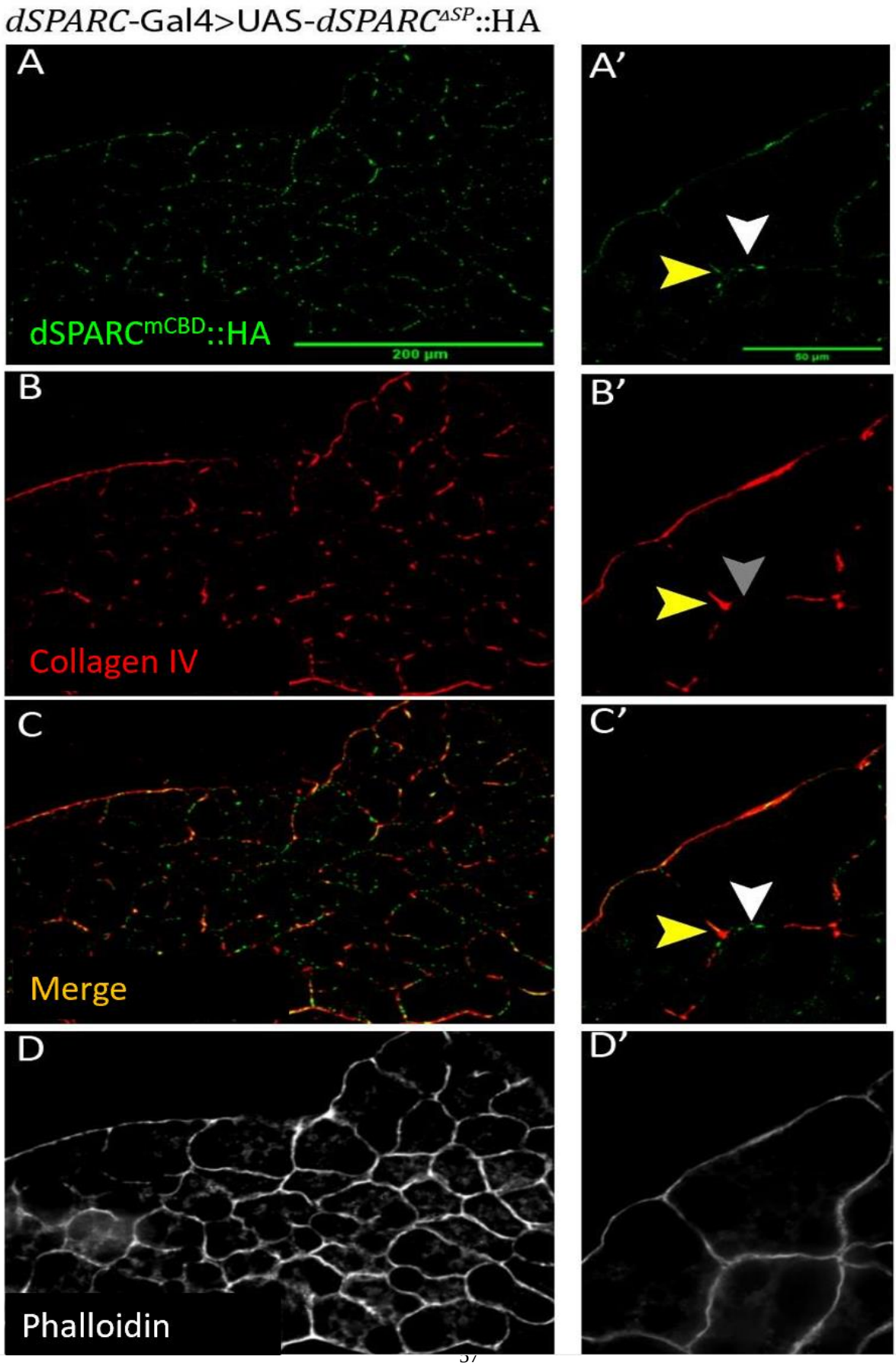
dSPARC-Gal4>UAS-dSPARC^ΔSP::HA
A
A'
dSPARC^mCBD::HA
200 µm
50 µm
B
B'
Collagen IV
C
C'
Merge
D
D'
Phalloidin

**Figure 15. Immunolocalization of cytosolic *dSPARC*$^{\Delta SP}$::HA in 3rd instar fat body.**

**A.** Detection of dSPARC-Gal4>*dSPARC*$^{\Delta SP}$::HA in a wild-type background with anti-HA antibody reveals putative cell border localization of *dSPARC*$^{\Delta SP}$::HA (white arrow), **(B)** anti-Cg25c reveals Collagen IV CIVICs localization (white arrow), with the grey arrow indicating a concentration of *dSPARC*$^{\Delta SP}$::HA outside of CIVICs. **C.** Merged images of A and B. **D.** Phalloidin staining.

*dSPARC*-Gal4>UAS-*hSPARC*$^{hSP}$*::HA*

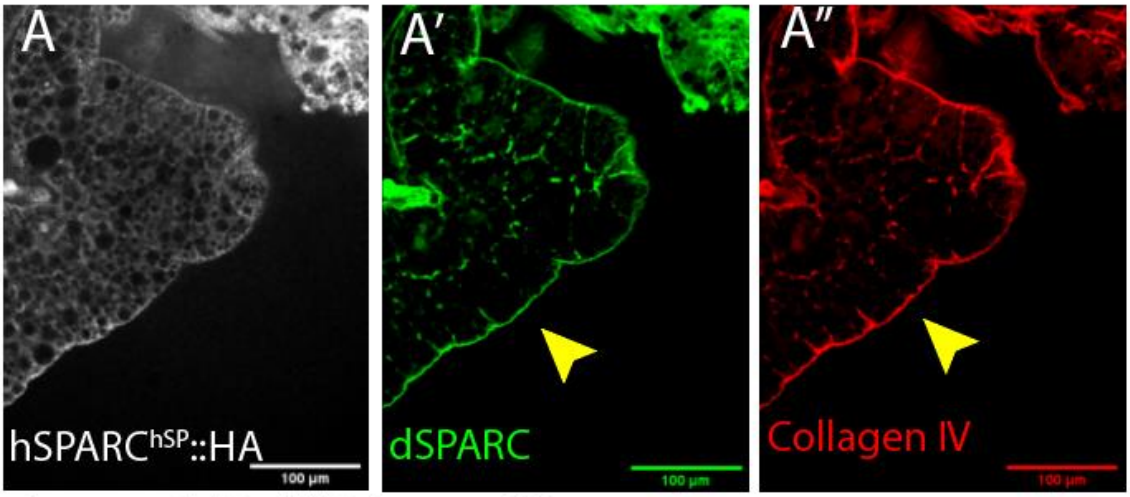


*dSPARC*-Gal4>UAS-*hSPARC*$^{dSP}$*::HA*

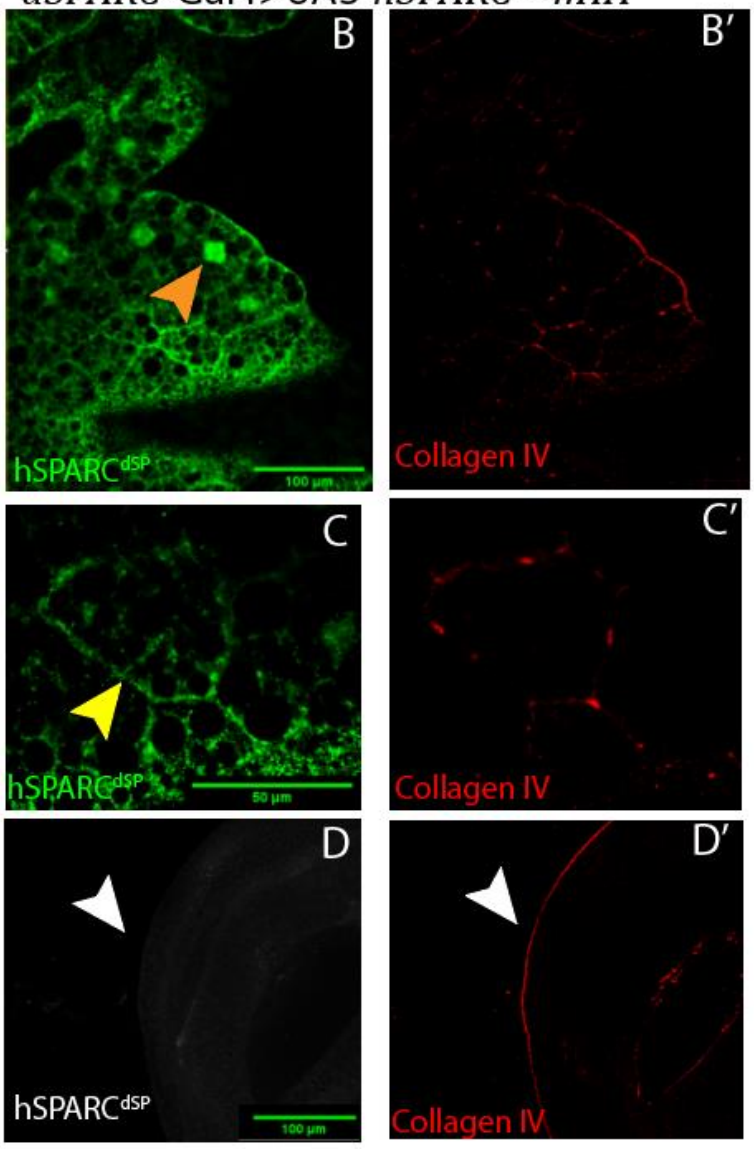

**Figure 16. Transgenic hSPARChSP::HA fails to localize to the fat body BM, whereas of hSPARCdSP::HA localizes at cell border and nuclei of adipocytes.**

**A.** Transgenic expression of *hSPARC*$^{hSP}$::HA shows weak staining when probed with anti-HA antibody in adipocytes. **A'-A''.** anti-dSPARC and anti-Cg25c antibody staining show concentrations in CIVICs and BM (Yellow arrow). **B-C.** Fat body immunostaining with anti-hSPARC antibody reveals nuclear (orange arrow) and cell border concentrations (yellow arrow) of *dSPARC*-Gal4>*hSPARC*$^{dSP}$::HA. **B'-C'.** Staining with anti-Cg25c antibody shows the presence of CIVICs structures. **D.** *dSPARC-Gal4>hSPARC*$^{dSP}$::HA stained with anti-hSPARC antibody showed no localization of *hSPARC*$^{dSP}$::HA to the wing imaginal disc BM, with anti-Cg-25c indicating the location of the BM (white arrow).

| Genotype | In WT background | In dSPARC-mutant background (dSPARC-Gal4/dSPARC$^{1510D}$) |
|---|---|---|
| *dSPARC::HA* | - Decreased Collagen IV solubility in the fat body.<br>- localizes to the wing imaginal disc BM. | Rescues 2$^{nd}$ instar lethality. |
| *dSPARC$^{\Delta SP}$::HA* | - No effect on Collagen IV.<br>- localizes in adipocyte cortex | Fails to rescue to adulthood. |
| *hSPARC$^{dSP}$::HA* | - No effect on Collagen IV.<br>-localizes in adipocyte periphery.<br>- did not localize in the wing imaginal disc BM. | Fails to rescue to adulthood. |
| *hSPARC$^{hSP}$::HA* | -No effect on Collagen IV.<br>- no visible concentration. | Fails to rescue to adulthood. |
| *dSPARC$^{mCDB}$::HA* | - No effect on Collagen IV.<br>- localizes in adipocyte periphery.<br>- did not localize to the wing imaginal discs BM. | Fails to rescue to adulthood. |

**Table 3. SPARC-constructs in either a wild-type or *dSPARC*-mutant background and their associated phenotype or localization.** The corresponding construct was driven with *dSPARC*-Gal4 in either a wild-type or *dSPARC-mutant* background. Rescue experiments were carried out in crosses with 7 virgins and 7 males at least 3 times. Failure to rescue was determined by an absence of adults with the appropriate genotype (*dSPARC*$^{1510D}$ /*dSPARC*-Gal4>SPARC construct).

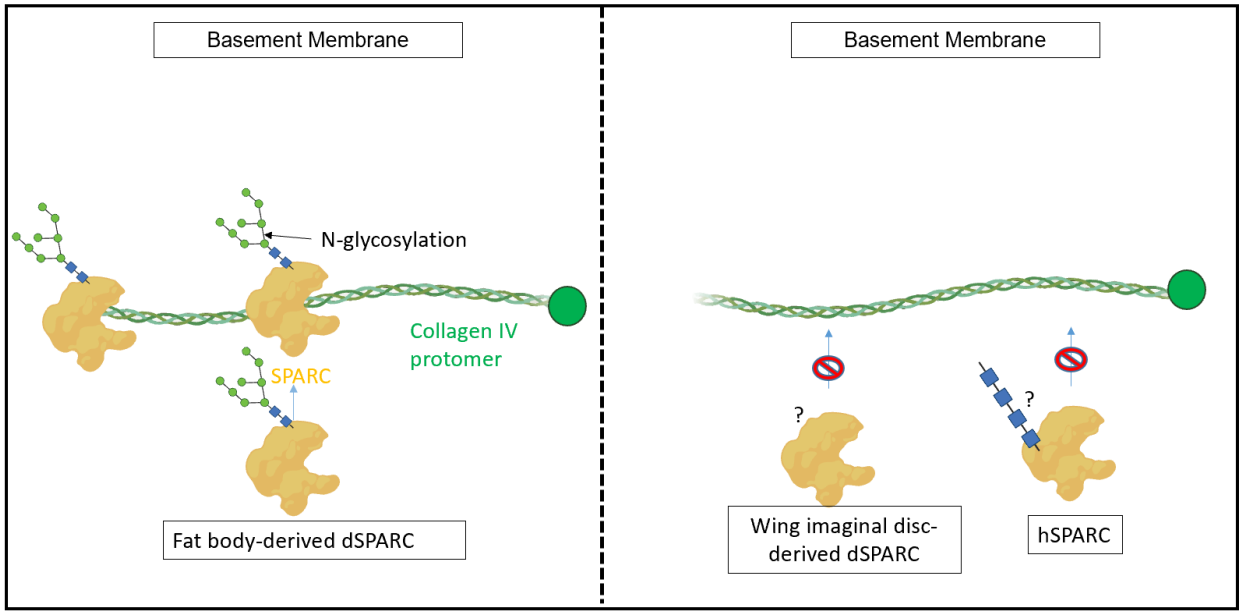
Basement Membrane
N-glycosylation
Collagen IV
protomer
SPARC
Fat body-derived dSPARC
Basement Membrane
?
?
Wing imaginal disc-
derived dSPARC
hSPARC

**Figure 17. Model of SPARC isoforms association with Collagen IV in BM.**

**A.** Fat body-derived dSPARC binds to Collagen IV. **B**. hSPARC and wing imaginal discs-derived dSPARC do not co-localize with Collagen IV in BM. The 67 kDa iSPARC is not illustrated as it is likely retained intracellularly.

# 5 Discussion

In invertebrates, SPARC is widely regarded as an extracellular Collagen-binding matricellular glycoprotein that is concentrated in BM. My data has revealed that in *Drosophila,* the ability of dSPARC (37 kDa) to localize to BMs is dependent on its tissue of origin. While fat body-derived dSPARC is concentrated within BMs, an isoform derived from imaginal wing discs forms no association with wing imaginal discs or fat body BM. Restricting dSPARC translation to the cytosol yields a high molecular weight protein (67 kDa) that phenocopies the size of a minor isoform observed with endogenous dSPARC. Moreover, intracellular dSPARC (idSPARC) is restricted to cell-cell borders rather than associated with BMs. Intriguingly, transgenic expression of hSPARC, with the presence of its native human signal peptide, also primarily yields a 67 kDa protein product, raising the possibility that like idSPARC, hSPARC is predominantly translated in the cytosol. My structure-function analyses data suggest that fat body BM fibrosis is not the underlying cause of larvae lethality. However, BM homeostasis at proximal and distal sites is dependent on the conservation of both the Collagen-binding epitopes and the disulfide bridge of EF-hand2 of fat body-derived dSPARC.

dSPARC mainly co-localizes in the fat body with Collagen IV in BM and CIVICs, with a some adipocyte pericellular distribution. The data indicate that the localization of a subset of dSPARC is thus independent of Collagen IV-rich ECMs. An unexpected finding is that wing imaginal disc-derived dSPARC does not associate with the BMs of either fat body or wing imaginal discs. This raises the possibility that dSPARC undergoes different posttranslational modifications in the fat body and wing imaginal disc, the latter likely dramatically reducing the affinity of dSPARC for Collagen IV. A precedent for this hypothesis is a report that differential N-glycosylation has been reported for bone- and platelet-derived hSPARC, with high mannose and complex glycosylation, respectively. Platelet-derived SPARC has no measurable Collagen affinity compared to bone-derived SPARC (Kelm and Mann, 1991). It is therefore conceivable that wing imaginal disc-derived dSPARC undergoes a form of N-glycosylation that negates its ability to bind to Collagen IV. Consistent with this hypothesis is that driving transgenic expression of mutated *dSPARC*$^{mCBD}$, both in the fat body and imaginal wing disc, phenocopies the distribution of imaginal wing disc-derived dSPARC in the pericellular domain of fat body adipocytes.

Despite the striking evolutionary conservation of the Collagen binding epitopes and disulfide-bridge EF-hand2 of SPARC, it was surprising that hSPARC could not rescue larvae lethality in the absence of dSPARC. Our laboratory previously reported, by immunohistochemistry and immuno-gold labeling, an intracellular association of SPARC with the 9+2 microtubule arrays of cilia on the surface ectoderm of *Xenopus* embryos(Huynh *et al.*, 2004). Moreover, using pull-down technology, we demonstrated that SPARC binds to tubulin (Huynh *et al.*, 2004). As noted above, when dSPARC translation in the fat body is restricted to the cytoplasm (iSPARC) by the absence of a signal peptide, it is concentrated pericellularly in adipocytes, a distribution that mirrors reported for *D*-syndecan, Rhea (talin) and IlK (integrin-linked kinase) (Dai et al., 2017). Moreover, iSPARC had a molecular weight of 67 kDa compared to the 37 kDa of secreted dSPARC. The approximate doubling in molecular weight is likely the result of post-translational cytosolic modifications, such as covalent fusion to an unknown protein and SUMOylation. A band of 67 kDa is also consistently observed by Western blot analyses of *Drosophila* S2 and vertebrate cell lysates (unpublished data). Unexpectedly, attempts to rescue the absence of dSPARC with a *hSPARC*$^{hSP}$::HA construct also mostly yielded a 67 kDa protein. However, unlike iSPARC, the putative cytosolic *hSPARC*$^{hSP}$*::*HA did not concentrate pericellularly in adipocyte. Futatsumori-Sugai and Tsumoto (2010) reported that silkworm cells poorly secrete human interleukin constructs unless the interleukins SP are exchanged for silkworm SP. They hypothesized that decreased secretion levels were due to poor translation of the cognate mRNAs. An alternative explanation is that the intracellular retention of hSPARC is caused by a poor recognition of the human SP sequence by *Drosophila* SRP. Consequently, cytosolic translation of the hSPARC$^{hSP}$ mRNA occurs uninterrupted to a length when binding of SPR can no longer effectively block translation in the cytosol. This likelihood is supported by the loss of the cytosolic 67 kDa protein band when the human signal peptide (*hSPARC*$^{hSP}$::HA) was substituted for the *Drosophila* SPARC signal peptide (*hSPARC*$^{dSP}$). Interestingly, the *hSPARC*$^{dSP}$ transgene was still unable to rescue *dSPARC* protein-null flies. Moreover, the resultant *hSPARC*$^{hSP}$::HA hybrid protein, like *dSPARC*$^{mCBD}$::HA was concentrated pericellularly on adipocytes and not within the BMs of fat body and wing imaginal discs. While it is unlikely that *hSPARC*$^{dSP}$ is also retained intracellularly, this possibility cannot conclusively be eliminated. Collectively, the data may be indicative of an interspecies conservation of SPARC function that is independent of BM assembly.

SPARC regulation of Collagen IV homeostasis was hypothesized to begin with an intracellular association with Collagen IV prior to their secretion. A chaperone-like activity was proposed that upon co-secretion, SPARC would inhibit Collagen IV binding to integrins, thereby delaying adequately Collagen IV nucleation to permit a sub-set of Collagen IV to assemble in the BM of distal tissues in 3rd instar larval. I now report that compared to 3rd instar wild type larval, where Collagen IV-positives vesicles are not readily visible by immunohistochemistry, 2nd instar adipocytes contain large numbers of Collagen IV-positive vesicle-like structures. Additionally, these structures increased dramatically in size in the absence of dSPARC, indicative of a large aberrant intracellular accumulation of Collagen IV, a phenomenon not observed with Laminin. The intracellular Collagen IV accumulation could be attributed to either a lack of secretion or an increase in endocytosis of Collagen IV. However, endocytosis is unlikely to be the main cause since intracellular vesicular accumulation of both secretion-competent *dSPARC*$^{mCBD}$::HA and Collagen IV is observed. Additionally, since *dSPARC*$^{mCBD}$::HA does not bind to Collagen IV and is absent from BM, they would not be expected to co-localize in structures by endocytosis. An issue that needs to be resolved is why *dSPARC*$^{mCBD}$::HA, which does not bind to Collagen IV, is able to co-localize in intracellular vesicle-like structures. This raises the possibility of an unknown intracellular mechanism or protein(s) which promotes their co-secretion. Another issue is why Collagen IV is not retained intracellularly by the knockdown of dSPARC in a 3rd instar fat body. It is possible that this phenomenon is more pronounced when intracellular trafficking of Collagen IV is most intense, such as observed with 2nd instar larval. I propose that, similar to the Collagen-specific chaperone HSP-47, dSPARC also acts as a Collagen IV chaperone that inhibits aberrant Collagen IV intracellular nucleation and/or polymerization. Whereas HSP-47 prevents Collagen IV protomer polymerization in the ER and during transit to the cis Golgi, unpublished data reported by Alexa Chioran in her M.Sc. thesis (Chioran, 2017) presents evidence that the Collagen IV chaperone-like activity is likely to commence in the trans Golgi network.

Transgenic expression of dSPARC$^{mCBD}$ in a dSPARC protein-null background (*dSPARC*$^{mCBD}$::HA;*dSPARC*$^{1510D}$/*dSPARC*-Gal4) compared to a *dSPARC*-null (+;*dSPARC*$^{1510D}$/*dSPARC*-Gal4) showed similar 2nd instar larval lethality phenotypes. However, transgenic expression of *dSPARC*$^{mCDB}$::HA in the fat body in a *dSPARC*-null background resulted in a milder rounding of adipocytes and less fibrotic BM compared to the complete absence of dSPARC (*dSPARC*$^{1510D}$). The data raises the possibility that *dSPARC*$^{mCBD}$::HA has only a

decrease, rather than a complete abolishment, of a binding affinity for Collagen IV. Alternatively, *dSPARC*$^{mCBD}$::HA may inhibit Collagen IV polymerization via interactions with other proteins, such as integrins. The latter possibility is supported by studies that vertebrate SPARC has a weak affinity for β1 integrins. Consequently, the presence of extracellular *dSPARC*$^{mCBD}$::HA would still promote indirectly Collagen IV solubility by masking integrins accesses to Collagen IV. For this proposed mechanism to be feasible, it is critical that dSPARC has only a weak affinity for *Drosophila* integrins, as reported with vertebrate SPARC, compared to its direct interaction with Collagen IV.

Biochemical studies with mammalian SPARC have reported that the disulfide bridge of EF-hand2 augments the affinity of SPARC for $Ca^{2+}$ which in turn enhances Collagen binding. Interestingly, transgenic expression dSPARC missing its EF-hand2 disulfide bridge (*dSPARC*$^{mDB}$::HA) rescued *dSPARC*-null flies with no overt adult phenotype. However, the 3$^{rd}$ instar fat bodies displayed a fibrotic-like accumulation of BM components that was strikingly similar to that observed in the fat body of dSPARC knockdown by RNAi (Shahab et al., 2015). It can therefore be concluded that larvae lethality is not due to a loss of larvae fat body BM homeostasis, but perhaps a loss of Collagen IV homeostasis in other tissues since *dSPARC*$^{mCBD}$::HA is lethal. In support of this supposition, knockdown of Collagen IV during embryogenesis leads to late embryonic lethality, characterized by muscle detachment of the embryonic heart tube (Hollfelder et al., 2014). Similar to the loss of dSPARC, a subset of Collagen mutants survived to 2$^{nd}$ instar. Larval development is not dependent on Collagen IV, but is required for pupal metamorphosis (Zajac and Horne-Badovinac, 2017). I propose that one possibility is that larvae lethality associated with an absence of dSPARC is the result of defective morphoregulatory events that could have been initiated during embryogenesis. It is conceivable that this defect(s) would not be lethal until 2$^{nd}$ instar, when the larvae is undergoing much higher biomechanical stress due to muscle and heart contractions. While speculative, my preliminary results indicate that knockdown of dSPARC during embryogenesis with a reintroduction of its expression in 1$^{st}$ larval stages, still results in larval lethality.

The aberrant accumulation of Collagen IV fibrils in the BM of fat body and wing imaginal discs observed by transgenic expression of *dSPARC*$^{mDB}$::HA in a *dSPARC* protein-null background could be attributed to several possibilities, such as: (1) an increase in Collagen IV synthesis or

secretion, (2) a decrease in Collagen IV endocytosis and/or (3), a decrease in solubility of Collagen IV in the hemolymph. All of which could individually or in concert lead to an aberrant Collagen IV polymerization. Presently, data from most studies lend greater support the hypothesis that dSPARC regulates Collagen IV nucleation at both proximal and distal sites by enhancing the solubility of Collagen IV prior to nucleation.

Overexpression of dSPARC results in a loss of 3$^{rd}$ instar fat body CIVICs, characterized by a decrease in adipocyte cell-cell adhesion (Dai et al., 2017). My data indicate that CIVICs are first detectable as larvae undergoing their transition from 2$^{nd}$ to 3$^{rd}$ instar, coincident 67-fold increase in adipocyte size. Our ultrastructural data indicate that dSPARC overexpression during the 2$^{nd}$ instar leads to mild changes in the surface topography of the adipocytes compared to a large decrease cell-cell adhesion observed in 3$^{rd}$ instar larvae. The milder overexpression phenotype in 2$^{rd}$ instar larvae is likely to be attributed to an insufficient level of Collagen IV in the BM. Thus, until late 2$^{nd}$ instar, the presence of a BM appears to be sufficient to maintain adipocyte cell-cell adhesion. By the time adipocytes have increased in size to a level observed in early 3$^{rd}$ instar, cell-cell adhesion appears co-dependent on the presence of CIVICs.

When *dSPARC$^{mCBD}$*::HA is expressed in wild-type background or a *dSPARC*-null background, dSPARC$^{mCBD}$::HA does not have a pericellular distribution with 2$^{nd}$ instar adipocytes, but is present at 3$^{rd}$ instar adipocyte surfaces. This raises the prospect that the adipocyte pericellular distribution of dSPARC is not fat body-derived. The pericellular localization is coincident with the onset of dSPARC expression by the imaginal wing discs. It is therefore plausible that wing imaginal discs dSPARC, which does not bind to Collagen IV, is the source of adipocyte pericellular dSPARC during 3$^{rd}$ instar development. dSPARC overexpression, which removes CIVICs cell-cell adhesion (Zajac and Horne-Badovinac, 2017), also leads to a loss of pericellular dSPARC on adipocytes. Thus, indicating that the wing imaginal disc-derived dSPARC requires adipocyte cell-cell adhesion for its proper localization. It remains to be established whether the pericellular dSPARC in adipocytes has functional significance, since the loss of imaginal wing disc-derived dSPARC shows no overt phenotype.

I propose an *in vivo* model on how SPARC regulates Collagen IV assembly and stability in BM. Key to this model is the identification of 4 putative binding sites on Collagen IV protomers (Chioran *et al.,* 2017). Overexpression of integrins in the fat body phenocopies *dSPARC*-null

phenotype (Dai et al., 2017). It is thereby feasible that a subset of SPARC bound to Collagen IV would diminish the binding of Collagen IV to integrins. Moreover, SPARC bound to the putative binding within the 7S domain would be expected to sterically interfere with the formation of antiparallel 7S tetramers. Thus, sterically interference with integrin binding and 7S tetramerization could act in concert to increase the solubility of Collagen IV protomers, thereby preventing premature polymerization intracellularly and extracellularly.

# 6 Future Directions

Different isoforms of dSPARC appear to be expressed depending on tissue origin and site of translation; i.e., fat body, wing discs and intracellular dSPARC (iSPARC). We are currently using a modified co-immunoprecipitation procedure to isolate isoforms for mass spectrometry for protein sequence and glycosylation analyses. Additionally, co-IP will also be uses in *dSPARC*$^{mCBD}$::HA and iSPARC to look for BM-independent and cytosolic protein-protein interactions.

It remains to be established why dSPARC and hSPARC have pericellular distributions on adipocytes that are distinct from Collagen IV-rich matrices. If differences in glycosylation are observed between fat body-derived hSPARC and dSPARC, transgenic constructs with different domain combinations of dSPARC and hSPARC will be generated to determine (1) which interspecies hybrids can rescue a loss of dSPARC and (2) which domains are responsible for Collagen IV-rich matrix independent localization.

For reasons that are still poorly understood, fat body BM fibrosis associated with loss of dSPARC is not larval lethal. It remains to be investigated whether the loss of dSPARC during embryogenesis results in embryonic defects that are exhibited during larval development. Hence, this would help ascertained if the knockdown of dSPARC from the onset of larval development results in larval lethality. If the data indicate that larval lethality is triggered by the absence of dSPARC during embryogenesis, the morphological impact on tissues other than the fat body will be examined, such as the heart, since Collagen IV mutants have embryonic and larvae heart defects (Hollfelder, Frasch, & Reim, 2014).

BM pores are observed at an ultrastructural level in the BMs of fat body of wild-type flies, likely serving as conduits for lipid vesicle diffusion into the hemolymph. A dramatic increase in the number and diameter of the pores was observed by the knockdown or mutations of dSPARC. One possibility, is that pore formation, is in part dependent of the dynamic interactions of dSPARC and Collagen IV with integrins. Hence, it should be determined whether pore formation is affected by knockdown or overexpression of integrins in the fat body adipocytes during larval development.

# References


Aguila, J. R. *et al.* (2007) 'The role of larval fat cells in adult Drosophila melanogaster', *Journal of Experimental Biology*. doi: 10.1242/jeb.001586.

Beira, J. V. and Paro, R. (2016) 'The legacy of Drosophila imaginal discs', *Chromosoma*. doi: 10.1007/s00412-016-0595-4.

Britton, J. S. and Edgar, B. A. (1998) 'Environmental control of the cell cycle in Drosophila: nutrition activates mitotic and endoreplicative cells by distinct mechanisms.', *Development (Cambridge, England)*. doi: 10.1007/s00227-002-0819-4.

Butterworth, F. M., Emerson, L. and Rasch, E. M. (1988) 'Maturation and degeneration of the fat body in the Drosophila larva and pupa as revealed by morphometric analysis', *Tissue and Cell*. doi: 10.1016/0040-8166(88)90047-X.

Chioran, A. *et al.* (2017) 'Collagen IV trafficking: The inside-out and beyond story', *Developmental Biology*, pp. 124–133. doi: 10.1016/j.ydbio.2017.09.037.

Fitzgerald, M. C. and Schwarzbauer, J. E. (1998) 'Importance of the basement membrane protein SPARC for viability and fertility in Caenorhabditis elegans', *Current Biology*. doi: 10.1016/S0960-9822(07)00540-4.

Futatsumori-Sugai, M. and Tsumoto, K. (2010) 'Signal peptide design for improving recombinant protein secretion in the baculovirus expression vector system', *Biochemical and Biophysical Research Communications*. doi: 10.1016/j.bbrc.2009.11.167.

Hackl, H. *et al.* (2005) 'Molecular processes during fat cell development revealed by gene expression profiling and functional annotation.', *Genome Biol*. doi: 10.1186/gb-2005-6-13-r108.

Hollfelder, D., Frasch, M. and Reim, I. (2014) 'Distinct functions of the laminin β LN domain and collagen IV during cardiac extracellular matrix formation and stabilization of alary muscle attachments revealed by EMS mutagenesis in Drosophila', *BMC Developmental Biology*. doi: 10.1186/1471-213X-14-26.

Hoshizaki, D. *et al.* (1995) 'Identification of fat-cell enhancer activity in Drosophila melanogaster using P-element enhancer traps', *Genome*. doi: 10.1139/g95-065.

Hoshizaki, D. K. *et al.* (1994) 'Embryonic fat-cell lineage in Drosophila melanogaster', *Development*.

Huynh, M. H. *et al.* (2004) 'Interaction between SPARC and tubulin in Xenopus', *Cell and Tissue Research*. doi: 10.1007/s00441-004-0933-3.

Inoue, Y. and Hayashi, S. (2007) 'Tissue-specific laminin expression facilitates integrin-dependent association of the embryonic wing disc with the trachea in Drosophila', *Developmental Biology*. doi: 10.1016/j.ydbio.2006.12.022.

Kelm, R. J. and Mann, K. G. (1991) 'The collagen binding specificity of bone and platelet osteonectin is related to differences in glycosylation', *Journal of Biological Chemistry*.

Ma, M. *et al.* (2017) 'Basement Membrane Manipulation in Drosophila Wing Discs Affects Dpp Retention but Not Growth Mechanoregulation', *Developmental Cell*. doi: 10.1016/j.devcel.2017.06.004.

Pastor-Pareja, J. C. and Xu, T. (2011) 'Shaping Cells and Organs in Drosophila by Opposing Roles of Fat Body-Secreted Collagen IV and Perlecan', *Developmental Cell*, 21(2), pp. 245–256. doi: 10.1016/j.devcel.2011.06.026.

Pottgiesser, J. *et al.* (1994) 'Changes in calcium and collagen iv binding caused by mutations in the ef hand and other domains of extracellular matrix protein BM-40 (SPARC, osteonectin)', *Journal of Molecular Biology*. doi: 10.1006/jmbi.1994.1315.

Riechmann, V. *et al.* (1998) 'The genetic control of the distinction between fat body and gonadal mesoderm in Drosophila', *Development*.

Sam, S., Leise, W. and Hoshizaki, D. K. (1996) 'The serpent gene is necessary for progression through the early stages of fat-body development', *Mechanisms of Development*. doi: 10.1016/S0925-4773(96)00615-6.

Schneider, R. H. *et al.* (2012) 'Stress reduction in the secondary prevention of cardiovascular

disease: Randomized, controlled trial of transcendental meditation and health education in blacks', *Circulation: Cardiovascular Quality and Outcomes*, 5(6), pp. 750–758. doi: 10.1161/CIRCOUTCOMES.112.967406.

Shahab, J. *et al.* (2015) 'Loss of SPARC dysregulates basal lamina assembly to disrupt larval fat body homeostasis in Drosophila melanogaster', *Developmental Dynamics*, 244(4), pp. 540–552. doi: 10.1002/dvdy.24243.

Zajac, A. L. and Horne-Badovinac, S. (2017) 'Tissue Structure: A CIVICs Lesson for Adipocytes', *Current Biology*, pp. R1013–R1015. doi: 10.1016/j.cub.2017.08.029.

Arnoys, E. J., & Wang, J. L. (2007). Dual localization: Proteins in extracellular and intracellular compartments. Acta Histochemica. https://doi.org/10.1016/j.acthis.2006.10.002

Borchiellini, C., Coulon, J., & Le Parco, Y. (1996). The function of type IV collagen during Drosophila muscle development. Mechanisms of Development. https://doi.org/10.1016/S0003-4975(98)00979-5

Bradshaw, A. D. (2009). The role of SPARC in extracellular matrix assembly. Journal of Cell Communication and Signaling. https://doi.org/10.1007/s12079-009-0062-6

Brekken, R. A., & Sage, E. H. (2000). SPARC, a matricellular protein: at the crossroads of cellmatrix.Matrix Biology. https://doi.org/10.1016/S0945-053X(00)00105-0

Brown, T. J., Shaw, P. A., Karp, X., Huynh, M. H., Begley, H., & Ringuette, M. J. (1999). Activation of SPARC expression in reactive stroma associated with human epithelial ovarian cancer. Gynecologic Oncology. https://doi.org/10.1006/gyno.1999.5552

Chen, J., Wang, M., Xi, B., Xue, J., He, D., Zhang, J., & Zhao, Y. (2012). SPARC is a key regulator of proliferation, apoptosis and invasion in human ovarian cancer. PloS One. https://doi.org/10.1371/journal.pone.0042413

Chioran, A., Duncan, S., Catalano, A., Brown, T. J., & Ringuette, M. J. (2017). Collagen IV trafficking: The inside-out and beyond story. Developmental Biology. https://doi.org/10.1016/j.ydbio.2017.09.037

Cydzik, M., Abdul-Wahid, A., Park, S., Bourdeau, A., Bowden, K., Prodeus, A., … Gariépy, J.

(2015). Slow binding kinetics of Secreted protein, acidic, rich in cysteine-VEGF interaction limit VEGF activation of VEGF receptor 2 and attenuate angiogenesis. FASEB Journal, 29(8), 3493–3505. https://doi.org/10.1096/fj.15-271775

Dai, J., Estrada, B., Jacobs, S., Sánchez-Sánchez, B. J., Tang, J., Ma, M., … Martín-Bermudo, M.D. (2018). Dissection of Nidogen function in Drosophila reveals tissue-specific mechanisms of basement membrane assembly. PLOS Genetics. https://doi.org/10.1371/journal.pgen.1007483

Dai, J., Ma, M., Feng, Z., & Pastor-Pareja, J. C. (2017). Inter-adipocyte Adhesion and Signaling byCollagen IV Intercellular Concentrations in Drosophila. Current Biology, 27(18), 2729-740.e4. https://doi.org/10.1016/j.cub.2017.08.002

Danysh, B. P., & Duncan, M. K. (2009). The lens capsule. Experimental Eye Research.https://doi.org/10.1016/j.exer.2008.08.002

Domogatskaya, A., Rodin, S., & Tryggvason, K. (2012). Functional Diversity of Laminins. Annual

Review of Cell and Developmental Biology. https://doi.org/10.1146/annurevcellbio-101011-

155750 Egeblad, M., & Werb, Z. (2002). New functions for the matrix metalloproteinases in cancer progression. Nature Reviews Cancer. https://doi.org/10.1038/nrc745

Fitzgerald, M. C., & Schwarzbauer, J. E. (1998). Importance of the basement membrane protein SPARCfor viability and fertility in Caenorhabditis elegans. Current Biology. https://doi.org/10.1016/S0960-9822(07)00540-4

Futatsumori-Sugai, M., & Tsumoto, K. (2010). Signal peptide design for improving recombinantprotein secretion in the baculovirus expression vector system. Biochemical and Biophysical Research Communications. https://doi.org/10.1016/j.bbrc.2009.11.167

Gilmour, D. T., Lyon, G. J., Carlton, M. B. L., Sanes, J. R., Cunningham, J. M., Anderson, J. R.,… Colledge, W. H. (1998). Mice deficient for the secreted glycoprotein SPARC/osteonectin/BM40 develop normally but show severe age-onset cataract formationand

disruption of the lens. EMBO Journal. https://doi.org/10.1128/JB.182.23.67426750.2000

Gubbiotti, M. A., Neill, T., & Iozzo, R. V. (2017). A current view of perlecan in physiology and pathology: A mosaic of functions. Matrix Biology. https://doi.org/10.1016/j.matbio.2016.09.003

Guo, H. F., Tsai, C. L., Terajima, M., Tan, X., Banerjee, P., Miller, M. D., … Kurie, J. M. (2018). Pro-metastatic collagen lysyl hydroxylase dimer assemblies stabilized by Fe2+binding. Nature Communications. https://doi.org/10.1038/s41467-018-02859-z

Guo, X., Johnson, J. J., & Kramer, J. M. (1991). Embryonic lethality caused by mutations in basement membrane collagen of C. elegans. Nature. https://doi.org/10.1038/349707a0

Gupta, M. C., Graham, P. L., & Kramer, J. M. (1997). Characterization of α1(IV) collagen mutations in Caenorhabditis elegans and the effects of α1 and α2(IV) mutations on type IV Collagen distribution. Journal of Cell Biology. https://doi.org/10.1083/jcb.137.5.1185

Hagedorn, E. J., & Sherwood, D. R. (2011). Cell invasion through basement membrane: The anchor cell breaches the barrier. Current Opinion in Cell Biology. https://doi.org/10.1016/j.ceb.2011.05.002

Hohenester, E., Sasaki, T., Giudici, C., Farndale, R. W., & Bächinger, H. P. (2008). Structural basis of sequence-specific collagen recognition by SPARC. Proceedings of the National Academyof Sciences of the United States of America, 105(47), 18273–18277. https://doi.org/10.1073/pnas.0808452105

Hollfelder, D., Frasch, M., & Reim, I. (2014). Distinct functions of the laminin β LN domain and collagen IV during cardiac extracellular matrix formation and stabilization of alary muscle attachments revealed by EMS mutagenesis in Drosophila. BMC Developmental Biology. https://doi.org/10.1186/1471-213X-14-26

Huynh, M. H., Sodek, K., Lee, H., & Ringuette, M. (2004). Interaction between SPARC and tubulin in Xenopus. Cell and Tissue Research. https://doi.org/10.1007/s00441-004-0933-3

Huynh, M. H., Zhu, S. J., Kollara, A., Brown, T., Winklbauer, R., & Ringuette, M. (2011). Knockdown of SPARC leads to decreased cell-cell adhesion and lens cataracts during

postgastrula development in Xenopus laevis. Development Genes and Evolution. https://doi.org/10.1007/s00427-010-0349-x

Isabella, A. J., & Horne-Badovinac, S. (2015). Dynamic regulation of basement membrane protein levels promotes egg chamber elongation in Drosophila. Developmental Biology. https://doi.org/10.1016/j.ydbio.2015.08.018

Jayadev, R., & Sherwood, D. R. (2017). Basement membranes. Current Biology. https://doi.org/10.1016/j.cub.2017.02.006

Kalluri, R. (2003). Basement membranes: Structure, assembly and role in tumour angiogenesis.Nature Reviews Cancer. https://doi.org/10.1038/nrc1094

Kelemen-Valkony, I., Kiss, M., Csiha, J., Kiss, A., Bircher, U., Szidonya, J., … Mink, M. (2012). Drosophila basement membrane collagen col4a1 mutations cause severe myopathy. Matrix Biology. https://doi.org/10.1016/j.matbio.2011.09.004

Kelley, L. C., Lohmer, L. L., Hagedorn, E. J., & Sherwood, D. R. (2014). Traversing the basement membrane in vivo: A diversity of strategies. Journal of Cell Biology. https://doi.org/10.1083/jcb.201311112

Kiss, M., Kiss, A. A., Radics, M., Popovics, N., Hermesz, E., Csiszár, K., & Mink, M. (2016). Drosophila type IV collagen mutation associates with immune system activation and intestinal dysfunction. Matrix Biology. https://doi.org/10.1016/j.matbio.2015.09.002

Koehler, A., Desser, S., Chang, B., MacDonald, J., Tepass, U., & Ringuette, M. (2009). Molecular evolution of SPARC: Absence of the acidic module and expression in the endoderm of the starlet sea anemone, Nematostella vectensis. Development Genes and Evolution. https://doi.org/10.1007/s00427-009-0313-9

Koide, T., Takahara, Y., Asada, S., & Nagata, K. (2002). Xaa-Arg-Gly triplets in the collagen triple helix are dominant binding sites for the molecular chaperone HSP47. Journal of Biological Chemistry. https://doi.org/10.1074/jbc.M106497200

Kuo, D. S., Labelle-Dumais, C., & Gould, D. B. (2012). Col4a1 and col4a2 mutations and disease: Insights into pathogenic mechanisms and potential therapeutic targets. Human

Molecular Genetics. https://doi.org/10.1093/hmg/dds346

Lane, T. F., & Sage, E. H. (1994). The biology of SPARC, a protein that modulates cell-matrix interactions. FASEB Journal. https://doi.org/10.1096/FASEBJ.8.2.8119487

Ledda, F., Bravo, A. I., Adris, S., Bover, L., Mordoh, J., & Podhajcer, O. L. (1997). The expression of the secreted protein acidic and rich in cysteine neoplastic progression of human melanoma. Journal of Investigative Dermatology. https://doi.org/10.1111/1523-1747.ep12334263

Li, S., Qi, Y., McKee, K., Liu, J., Hsu, J., & Yurchenco, P. D. (2017). Integrin and dystroglycan compensate each other to mediate laminin-dependent basement membrane assembly and epiblast polarization. Matrix Biology. https://doi.org/10.1016/j.matbio.2016.07.005

Lindner, J. R., Hillman, P. R., Barrett, A. L., Jackson, M. C., Perry, T. L., Park, Y., & Datta, S. (2007). The Drosophila Perlecan gene trol regulates multiple signaling pathways in different developmental contexts. BMC Developmental Biology. https://doi.org/10.1186/1471-213X-7-121

Martinek, N., Shahab, J., Saathoff, M., & Ringuette, M. (2011). Haemocyte-derived SPARC is required for collagen-IV-dependent stability of basal laminae in Drosophila embryos. Journal of Cell Science. https://doi.org/10.1242/jcs.086819

Martinek, N., Zou, R., Berg, M., Sodek, J., & Ringuette, M. (2002). Evolutionary conservation and association of SPARC with the basal lamina in Drosophila. Development Genes and Evolution. https://doi.org/10.1007/s00427-002-0220-9

Maurer, P., Hohenadl, C., Hohenester, E., Göhring, W., Timpl, R., & Engel, J. (1995). The Cterminal portion of BM-40 (SPARC/osteonectin) is an autonomously folding and crystallisable domain that binds calcium and collagen IV. Journal of Molecular Biology,253, 347–357. https://doi.org/10.1006/jmbi.1995.0557

Mayer, U., Aumailley, M., Mann, K., Timpl, R., & Eengel, J. (1991). Calcium-dependent binding of basement membrane protein BM-40 (osteonectin, SPARC) to basement membrane

collagen type IV. European Journal of Biochemistry.https://doi.org/10.1111/j.1432-1033.1991.tb15996.x

Medioni, C. (2005). Dynamics of the basement membrane in invasive epithelial clusters in Drosophila. Development. https://doi.org/10.1242/dev.01886

Morrissey, M. A., Jayadev, R., Miley, G. R., Blebea, C. A., Chi, Q., Ihara, S., & Sherwood, D. R. (2016). SPARC Promotes Cell Invasion In Vivo by Decreasing Type IV Collagen Levels in the Basement Membrane. PLoS Genetics, 12(2). https://doi.org/10.1371/journal.pgen.1005905

Norose, K., Clark, J. I., Syed, N. A., Basu, A., Heber-Katz, E., Sage, E. H., & Howe, C. C. (1998). SPARC deficiency leads to early-onset cataractogenesis. Investigative Ophthalmology and Visual Science.

Nozaki, M., Sakurai, E., Raisler, B. J., Baffi, J. Z., Witta, J., Ogura, Y., … Ambati, J. (2006). Loss of SPARC-mediated VEGFR-1 suppression after injury reveals a novel antiangiogenic activity of VEGF-A. Journal of Clinical Investigation. https://doi.org/10.1172/JCI26316

Ono, T., Miyazaki, T., Ishida, Y., Uehata, M., & Nagata, K. (2012). Direct in vitro and in vivo evidence for interaction between Hsp47 protein and collagen triple helix. Journal of Biological Chemistry. https://doi.org/10.1074/jbc.M111.280248

Pastor-Pareja, J. C., & Xu, T. (2011). Shaping Cells and Organs in Drosophila by OpposingRoles of Fat Body-Secreted Collagen IV and Perlecan. Developmental Cell, 21(2), 245–256. https://doi.org/10.1016/j.devcel.2011.06.026

Poschl, E. (2004). Collagen IV is essential for basement membrane stability but dispensable for initiation of its assembly during early development. Development. https://doi.org/10.1242/dev.01037

Pottgiesser, J., Maurer, P., Mayer, U., Nischt, R., Mann, K., Timpl, R., … Engel, J. (1994). Changes in calcium and collagen iv binding caused by mutations in the ef hand and other domains of extracellular matrix protein BM-40 (SPARC, osteonectin). Journal of Molecular Biology. https://doi.org/10.1006/jmbi.1994.1315

Rempel, S. A., Ge, S., & Gutiérrez, J. A. (1999). SPARC: A potential diagnostic marker of invasive meningiomas. Clinical Cancer Research.

Rentz, T. J., Poobalarahi, F., Bornstein, P., Sage, E. H., & Bradshaw, A. D. (2007). SPARC regulates processing of procollagen I and collagen fibrillogenesis in dermal fibroblasts. Journal of Biological Chemistry. https://doi.org/10.1074/jbc.M700167200

Ringuette, M., Drysdale, T., & Liu, F. (1992). Expression and distribution of SPARC in early Xenopus laevis embryos. Roux's Archives of Developmental Biology. https://doi.org/10.1007/BF00364591

Rowe, R. G., & Weiss, S. J. (2008). Breaching the basement membrane: who, when and how? Trends in Cell Biology. https://doi.org/10.1016/j.tcb.2008.08.007

Sasaki, T., Hohenester, E., Göhring, W., & Timpl, R. (1998). Crystal structure and mapping by site-directed mutagenesis of the collagen-binding epitope of an activated form of BM40/SPARC/osteonectin. EMBO Journal, 17(6), 1625–1634 https://doi.org/10.1093/emboj/17.6.1625

Schwarzbauer, J., & Spencer, C. (1993). The Caenorhabditis-elegans homolog of the extracellular calcium-binding protein SPARC/osteonectin affects nematode body morphology and mobility. Molecular Biology of the Cell. https://doi.org/10.1091/mbc.4.9.941

Shahab, J., Baratta, C., Scuric, B., Godt, D., Venken, K. J. T., & Ringuette, M. J. (2015). Loss of SPARC dysregulates basal lamina assembly to disrupt larval fat body homeostasis in Drosophila melanogaster. Developmental Dynamics, 244(4), 540–552. https://doi.org/10.1002/dvdy.24243

Sibley, M. H., Graham, P. L., von Mende, N., & Kramer, J. M. (1994). Mutations in the alpha 2(IV) basement membrane collagen gene of Caenorhabditis elegans produce phenotypes of differing severities. EMBO J.

Srivastava, A., Pastor-Pareja, J. C., Igaki, T., Pagliarini, R., & Xu, T. (2007). Basement membrane remodeling is essential for Drosophila disc eversion and tumor invasion. PNAS. https://doi.org/10.1073/pnas.0611666104

Tasab, M., Batten, M. R., & Bulleid, N. J. (2000). Hsp47: A molecular chaperone that interacts with and stabilizes correctly-folded procollagen. EMBO Journal. https://doi.org/10.1093/emboj/19.10.2204

Urbano, J. M., Domínguez-Giménez, P., Estrada, B., & Martín-Bermudo, M. D. (2011). PS integrins and laminins: Key regulators of cell migration during drosophila embryogenesis. PLoS ONE, 6(9). https://doi.org/10.1371/journal.pone.0023893

Werb, Z., & Chin, J. R. (1998). Extracellular matrix remodeling during morphogenesis. In Annals of the New York Academy of Sciences. https://doi.org/10.1111/j.17496632.1998.tb10111.x

Yan, Q., Clark, J. I., Wight, T. N., & Sage, E. H. (2002). Alterations in the lens capsule contribute to cataractogenesis in SPARC-null mice. Journal of Cell Science.

Yan, Q., Perdue, N., Blake, D., & Sage, E. H. (2005). Absence of SPARC in murine lens epithelium leads to increased deposition of laminin-1 in lens capsule. Investigative Ophthalmology and Visual Science. https://doi.org/10.1167/iovs.05-0460

Yasuhiro Matsuoka, Hiroshi Kubota, Eijiro Adachi, Naoko Nagai, Toshihiro Marutani, Nobuko

Hosokawa, K. N. (2004). Insufficient Folding of Type IV Collagen and Formation of Abnormal Basement Membrane-like Structure in Embryoid Bodies Derived from Hsp47Null Embryonic Stem Cells. Molecular Biology of the Cell. https://doi.org/10.1091/mbc.E04-01-0050

# 7 Appendices

## 7.1 Appendix 1

| Genotype | Description |
|---|---|
| Bl/Cyo; TM2/TM6B | Double balance line |
| En/Cyo; MRKS/TM6B | Engrail driver |
| *dSPARC*-Gal4/TM6B, GFP | dSPARC driver |
| *Cg*-Gal4/*Cg*-Gal4 | Cg 25c Driver |
| $dSPARC^{1510D}$/TM6B, GFP | *dSPARC*-mutant protein null |
| Bl/Cyo; Df(3R)136mn/TM6B | Def-dSPARC protein null |
| *dSPARC*::HA/ *dSPARC*::HA ; TM2/TM6B | dSPARC tagged with HA (II) |
| Bl/Cyo; UAS-*dSPARC*::HA/ UAS-*dSPARC*::HA | dSPARC tagged with HA (III) |
| Bl/Cyo; $dSPARC_{RNAI\text{-}16678}$ | RNAi against dSPARC |
| $Gal80^{ts}$;TM2/TM6B | Temperature sensitive Gal 80 |
| $dSPARC^{mCBD}$::HA | dSPARC construct with mutated collagen binding epitodes |
| $dSPARC^{\Delta Dis}$::HA | dSPARC construct missing the EF-hand-2 disulfide bridge |
| $dSPARC^{\Delta SP}$::HA | dSPARC missing a signal peptide |
| $hSPARC^{dSP}$ | Human SPARC with a drosophila signal peptide |
| $hSPARC^{hSP}$::HA | Human SPARC with a human signal peptide |

| | |
|---|---|
| *dSPARC*::GFP | dSPARC tagged with GFP |
| *Cg*-Gal4/*Cg*-Gal4; *dSPARC*::HA/UAS-*dSPARC*::HA | |
| *Cg*-Gal4/*Cg*-Gal4; *dSPARC*::HA/UAS-*dSPARC*::HA | |
| *dSPARC*::HA; *dSPARC*-gal4/ Def(3R) 136mn | |
| *dSPARC*::HA; *dSPARC*-gal4/ $dSPARC^{1510D}$ | |
| $dSPARC^{mCBD}$::HA; *dSPARC*-gal4/ $dSPARC^{1510D}$ | |
| $dSPARC^{\Delta Dis}$::HA; *dSPARC*-gal4/ $dSPARC^{1510D}$ | |
| $dSPARC^{\Delta SP}$::HA; *dSPARC*-gal4/ $dSPARC^{1510D}$ | |
| $hSPARC^{dSP}$; *dSPARC*-gal4/ $dSPARC^{1510D}$ | |
| $hSPARC^{hSP}$::HA; *dSPARC*-gal4/ $dSPARC^{1510D}$ | |
| *En*-Gal4/ *dSPARC*::HA | |
| *En*-Gal4/ $dSPARC^{mCBD}$::HA | |
| *En*-Gal4/ $dSPARC^{\Delta Dis}$::HA | |
| *dSPARC*::HA; *dSPARC*-gal4/ + | |
| $dSPARC^{mCBD}$::HA; *dSPARC*-gal4/ + | |
| $dSPARC^{\Delta SP}$::HA; *dSPARC*-gal4/ + | |
| $hSPARC^{dSP}$; *dSPARC*-gal4/ + | |
| $hSPARC^{hSP}$::HA; *dSPARC*-gal4/ + | |
| $dSPARC^{RNAi16678}$/ *dSPARC*-Gal4 | |
| $Gal80^{ts}$; $dSPARC^{RNAi-16678}$/ *dSPARC*-Gal4 | |

## 7.2 Appendix 2

Human SPARC Forward Primer

5’-CCAATTCAGTCGACCACCATGAGGGCCTGGATCT-3’

Human SPARC Reverse Primer

5’-TATGATGCGGCCGCACTACGATCACAAGATCCTTGTCGATATCC-3’

Human SPARC Middle Sequence Primer

5’-GAGAGGGATGAGGACAACA-3’

Drosophila SPARC Forward Primer

5’-ACCAATCCGGACAACGCGCA-3’

Drosophila SPARC Reverse Primer

5’-GATGTGCATGTGCGCGTTGT-3’

DNA sequences, vector sequences not included. Mutations and changes highlighted in red.

Human SPARC with human signal peptide

**ATG**AGGGCCTGGATCTTCTTTCTCCTTTGCCTGGCCGGGAGGGCCTTGGCAGCCCCT

CAGCAAGAAGCCCTGCCTGATGAGACAGAGGTGGTGGAAGAAACTGTGGCAGAGG

TGACTGAGGTATCTGTGGGAGCTAATCCTGTCCAGGTGGAAGTAGGAGAATTTGAT

GATGGTGCAGAGGAAACCGAAGAGGAGGTGGTGGCGGAAAATCCCTGCCAGAACC

ACCACTGCAAACACGGCAAGGTGTGCGAGCTGGATGAGAACAACACCCCCATGTG

CGTGTGCCAGGACCCCACCAGCTGCCCAGCCCCCATTGGCGAGTTTGAGAAGGTGT

GCAGCAATGACAACAAGACCTTCGACTCTTCCTGCCACTTCTTTGCCACAAAGTGCA

CCCTGGAGGGCACCAAGAAGGGCCACAAGCTCCACCTGGACTACATCGGGCCTTGC
AAATACATCCCCCCTTGCCTGGACTCTGAGCTGACCGAATTCCCCCTGCGCATGCGG

GACTGGCTCAAGAACGTCCTGGTCACCCTGTATGAGAGGGATGAGGACAACAACCT

TCTGACTGAGAAGCAGAAGCTGCGGGTGAAGAAGATCCATGAGAATGAGAAGCGC

CTGGAGGCAGGAGACCACCCCGTGGAGCTGCTGGCCCGGGACTTCGAGAAGAACT

ATAACATGTACATCTTCCCTGTACACTGGCAGTTCGGCCAGCTGGACCAGCACCCC

ATTGACGGGTACCTCTCCCACACCGAGCTGGCTCCACTGCGTGCTCCCCTCATCCCC

ATGGAGCATTGCACCACCCGCTTTTTCGAGACCTGTGACCTGGACAATGACAAGTA

CATCGCCCTGGATGAGTGGGCCGGCTGCTTCGGCATCAAGCAGAAGGATATCGACA
AGGATCTTGTGATCGTAGTGCGGCCGCACTCGAGATATCTAGACCCAGCTTTCTTGT

ACAAAGTGGTGAGATCTATGGTGAGCAAGGGCGAGGAGGATAACATGGCCATCAT

CAAGGAGTT CATGCGCTTCAAGGTGCACATGGAGGGCTCCGTGAACG

Human SPARC with *Drosophila* signal peptide

**ATG**CGCTCCCTTTGGCTGCTGCTCGGCTTGGGCCTGCTGGCTGTGAGCGCCCCTCAG

CAAGAAGCCCTGCCTGATGAGACAGAGGTGGTGGAAGAAACTGTGGCAGAGGTGA

CTGAGGTATCTGTGGGAGCTAATCCTGTCCAGGTGGAAGTAGGAGAATTTGATGAT

GGTGCAGAGGAAACCGAAGAGGAGGTGGTGGCGGAAAATCCCTGCCAGAACCACC

ACTGCAAACACGGCAAGGTGTGCGAGCTGGATGAGAACAACACCCCCATGTGCGT

GTGCCAGGACCCCACCAGCTGCCCAGCCCCCATTGGCGAGTTTGAGAAGGTGTGCA

GCAATGACAACAAGACCTTCGACTCTTCCTGCCACTTCTTTGCCACAAAGTGCACCC

TGGAGGGCACCAAGAAGGGCCACAAGCTCCACCTGGACTACATCGGGCCTTGCAA

ATACATCCCCCCTTGCCTGGACTCTGAGCTGACCGAATTCCCCCTGCGCATGCGGGA

CTGGCTCAAGAACGTCCTGGTCACCCTGTATGAGAGGGATGAGGACAACAACCTTC

TGACTGAGAAGCAGAAGCTGCGGGTGAAGAAGATCCATGAGAATGAGAAGCGCCT

GGAGGCAGGAGACCACCCCGTGGAGCTGCTGGCCCGGGACTTCGAGAAGAACTAT

AACATGTACATCTTCCCTGTACACTGGCAGTTCGGCCAGCTGGACCAGCACCCCATT

GACGGGTACCTCTCCCACACCGAGCTGGCTCCACTGCGTGCTCCCCTCATCCCCATG

GAGCATTGCACCACCCGCTTTTTCGAGACCTGTGACCTGGACAATGACAAGTACAT
CGCCCTGGATGAGTGGGCCGGCTGCTTCGGCATCAAGCAGAAGGATATCGACAAGG
ATCTTGTGATC**TAG**

*Drosophila* SPARC

**ATG**CGCTCCCTTTGGCTGCTGCTCGGCTTGGGCCTGCTGGCTGTGAGCCACGTCCAG

GCCTCTACGGAGTTTTCCGAAGATCTGCTGGATGAGGACCTCGACCTGTCCGACATC

GATGAGAACGAAGAGGAGTTCCTGCGCCTGCTGGAGGAGAAGAACAAGATCAAGG

ATATTGAGCGCGAGAATGAGATTGCCACCAAGCTGGCCGAAGTGCAGCACAATCTA

CTCAATCCCGTTGTCGAGGTGGATCTGTGCGAAACGATGAGCTGCGGAGCCGGTCG

CATCTGCCAGATGCACGACGAGAAGCCCAAATGCGTGTGCATTCCGGAGTGCCCGG
AGGAGGTGGACACTCGCCGCCTGGTCTGCACCAATACCAACGAGACCTGGCCGTCG

GACTGCTCTGTGTATCAGCAGCGCTGCTGGTGCGACAGCGGCGAGCCCGGCTGCAC

CAATCCGGACAACGCGCACATGCACATCGACTACTACGGCGCTTGCCACGAGCCCA

GGAGCTGCGAGGGCGAGGACCTGAAGGACTTCCCCAGGCGCATGCGCGACTGGCT

GTTCAACGTGATGCGCGACCTGGCCGAGCGCGACGAGCTGACCGAGCACTACATGC

AGATGGAGCTGGAGGCGGAGACCAACAACTCGCGTCGCTGGTCGAACGCCGCCGT

GTGGAAGTGGTGCGACCTGGACGGCGATACCGATCGCTCCGTCTCGCGCCACGAGC

TCTTCCCCATCCGTGCTCCGCTGGTCAGTCTCGAGCACTGCATCGCACCCTTCCTCG

AGTCCTGCGACTCCAACAAGGACCATCGCATCACCCTGGTGGAGTGGGGCGCCTGC

CTGGAGCTGGATCCCGAGGACCTCAAGGAGCGTTGCGACGACGTCCAGCGGGCTCA

GCCCCATCTTCTGGGTGCGGCGCGGCCGCACTCGAGATATCTAGACCCAGCTTTCTT

GTACAAAGTGGTGAGATCTATGGTGAGCAAGGGCGAGGAGGATAACATGGCCATC

ATCAAGGAGTT CATGCGCTTCAAGGTGCACATGGAGGGCTCCGTGAACG

*Drosophila* SPARC without signal peptide

**ATG**GCCTCTACGGAGTTTTCCGAAGATCTGCTGGATGAGGACCTCGACCTGTCCGA
CATCGATGAGAACGAAGAGGAGTTCCTGCGCCTGCTGGAGGAGAAGAACAAGATC

AAGGATATTGAGCGCGAGAATGAGATTGCCACCAAGCTGGCCGAAGTGCAGCACA

ATCTACTCAATCCCGTTGTCGAGGTGGATCTGTGCGAAACGATGAGCTGCGGAGCC

GGTCGCATCTGCCAGATGCACGACGAGAAGCCCAAATGCGTGTGCATTCCGGAGTG

CCCGGAGGAGGTGGACACTCGCCGCCTGGTCTGCACCAATACCAACGAGACCTGGC

CGTCGGACTGCTCTGTGTATCAGCAGCGCTGCTGGTGCGACAGCGGCGAGCCCGGC

TGCACCAATCCGGACAACGCGCACATGCACATCGACTACTACGGCGCTTGCCACGA

GCCCAGGAGCTGCGAGGGCGAGGACCTGAAGGACTTCCCCAGGCGCATGCGCGAC

TGGCTGTTCAACGTGATGCGCGACCTGGCCGAGCGCGACGAGCTGACCGAGCACTA

CATGCAGATGGAGCTGGAGGCGGAGACCAACAACTCGCGTCGCTGGTCGAACGCC

GCCGTGTGGAAGTGGTGCGACCTGGACGGCGATACCGATCGCTCCGTCTCGCGCCA

CGAGCTCTTCCCCATCCGTGCTCCGCTGGTCAGTCTCGAGCACTGCATCGCACCCTT

CCTCGAGTCCTGCGACTCCAACAAGGACCATCGCATCACCCTGGTGGAGTGGGGCG

CCTGCCTGGAGCTGGATCCCGAGGACCTCAAGGAGCGTTGCGACGACGTCCAGCGG

GCTCAGCCCCATCTTCTGGGTGCGGCGCGGCCGCACTCGAGATATCTAGACCCAGC

TTTCTTGTACAAAGTGGTGAGATCTATGGTGAGCAAGGGCGAGGAGGATAACATGG

CCATCATCAA GGAGTTCATGCGCTTCAAGGTGCACATGGAGGGCTCCGTG

*Drosophila* SPARC with mutated collagen binding residues

**ATG**CGCTCCCTTTGGCTGCTGCTCGGCTTGGGCCTGCTGGCTGTGAGCCACGTCCAG

GCCTCTACGGAGTTTTCCGAAGATCTGCTGGATGAGGACCTCGACCTGTCCGACATC

GATGAGAACGAAGAGGAGTTCCTGCGCCTGCTGGAGGAGAAGAACAAGATCAAGG

ATATTGAGCGCGAGAATGAGATTGCCACCAAGCTGGCCGAAGTGCAGCACAATCTA

CTCAATCCCGTTGTCGAGGTGGATCTGTGCGAAACGATGAGCTGCGGAGCCGGTCG

CATCTGCCAGATGCACGACGAGAAGCCCAAATGCGTGTGCATTCCGGAGTGCCCGG
AGGAGGTGGACACTCGCCGCCTGGTCTGCACCAATACCAACGAGACCTGGCCGTCG

GACTGCTCTGTGTATCAGCAGCGCTGCTGGTGCGACAGCGGCGAGCCCGGCTGCAC

CAATCCGGACAACGCGCACATGCACATCGACTACTACGGCGCTTGCCACGAGCCCA

GGAGCTGCGAGGGCGAGGACCTGAAGGACTTCCCCAGGCGC(>CTC)ATGCGCGACT

GGCTGTTCAACGTGATGCGCGACCTGGCCGAGCGCGACGAGCTGACCGAGCACTAC

ATGCAGATGGAGCTGGAGGCGGAGACCAACAACTCGCGTCGCTGGTCGAACGCCG

CCGTGTGGAAGTGGTGCGACCTGGACGGCGATACCGATCGCTCCGTCTCGCGCCAC

GAGCTCTTCCCCATCCGTGCTCCGCTGGTCAGTCTCGAG(>GCG)CACTGCATCGCAC

CCTTCCTCGAGTCCTGCGACTCCAACAAGGACCATCGCATCACCCTGGTGGAGTGG

GGCGCCTGCCTGGAGCTGGATCCCGAGGACCTCAAGGAGCGTTGCGACGACGTCCA

GCGGGCTCAGCCCCATCTTCTGGGTGCGGCGCGGCCGCACTCGAGATATCTAGACC

CAGCTTTCTTGTACAAAGTGGTGAGATCTATGGTGAGCAAGGGCGAGGAGGATAAC

ATGGCCAT CATCAAGGAGTTCATGCGCTTCAAGGTGCACATGGAGGGCTCCGTG

*Drosophila* SPARC without disulfide bond in EF hand II

ATGCGCTCCCTTTGGCTGCTGCTCGGCTTGGGCCTGCTGGCTGTGAGCCACGTCCAG

GCCTCTACGGAGTTTTCCGAAGATCTGCTGGATGAGGACCTCGACCTGTCCGACATC

GATGAGAACGAAGAGGAGTTCCTGCGCCTGCTGGAGGAGAAGAACAAGATCAAGG

ATATTGAGCGCGAGAATGAGATTGCCACCAAGCTGGCCGAAGTGCAGCACAATCTA

CTCAATCCCGTTGTCGAGGTGGATCTGTGCGAAACGATGAGCTGCGGAGCCGGTCG

CATCTGCCAGATGCACGACGAGAAGCCCAAATGCGTGTGCATTCCGGAGTGCCCGG
AGGAGGTGGACACTCGCCGCCTGGTCTGCACCAATACCAACGAGACCTGGCCGTCG

GACTGCTCTGTGTATCAGCAGCGCTGCTGGTGCGACAGCGGCGAGCCCGGCTGCAC

CAATCCGGACAACGCGCACATGCACATCGACTACTACGGCGCTTGCCACGAGCCCA

GGAGCTGCGAGGGCGAGGACCTGAAGGACTTCCCCAGGCGCATGCGCGACTGGCT

GTTCAACGTGATGCGCGACCTGGCCGAGCGCGACGAGCTGACCGAGCACTACATGC

AGATGGAGCTGGAGGCGGAGACCAACAACTCGCGTCGCTGGTCGAACGCCGCCGT

GTGGAAGTGGTGCGACCTGGACGGCGATACCGATCGCTCCGTCTCGCGCCACGAGC

TCTTCCCCATCCGTGCTCCGCTGGTCAGTCTCGAGCACTGCATCGCACCCTTCCTCG

AGTCCTGC(>GCC)GACTCCAACAAGGACCATCGCATCACCCTGGTGGAGTGGGGCG

CCTGC(>GCC)CTGGAGCTGGATCCCGAGGACCTCAAGGAGCGTTGCGACGACGTCC
AGCGGGCTCAGCCCCATCTTCTGGGTGCGGCGCGGCCGCACTCGAGATATCTAGAC

CCAGCTTTCTTGTACAAAGTGGTGAGATCTATGGTGAGCAAGGGCGAGGAGGATAA
CATGGCCATCATCAAGGAGTTCATGCGCTTCAAGGTGCACATGGAGGGCTCCGT